N O T I C E

THIS DOCUMENT HAS BEEN REPRODUCED FROM MICROFICHE. ALTHOUGH IT IS RECOGNIZED THAT CERTAIN PORTIONS ARE ILLEGIBLE, IT IS BEING RELEASED IN THE INTEREST OF MAKING AVAILABLE AS MUCH INFORMATION AS POSSIBLE

NASA
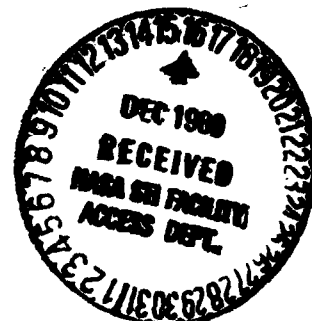
Technical Memorandum 82011

An Analysis of Short Pulse and Dual Frequency Radar Techniques for Measuring Ocean Wave Spectra from Satellites

Frederick C. Jackson

OCTOBER 1980

AN ANALYSIS OF SHORT PULSE AND DUAL FREQUENCY RADAR TECHNIQUES FOR MEASURING OCEAN WAVE SPECTRA FROM SATELLITES

Frederick C. Jackson

NASA/Goddard Space Flight Center
Greenbelt, Maryland 20/71

October 1980

ABSTRACT

We show how relatively simple, non-imaging, microwave radars can be used to measure ocean wave directional spectra from satellites. In the non-imaging radar measurement, the directional distribution of the ocean waves is obtained by scanning the radar in azimuth; the resolution of Fourier component waves in any given azimuth direction is a result of a Bragg type of wave front matching condition. The spectral distribution in wave number can in principle be measured using either short pulse (SP) or dual frequency (DF) techniques.

In this paper, we analyze the SP and DF techniques in the frequency domain, in which is evident a common dependence on a generalized fourth-order statistical moment of the surface scattering transfer function. A solution for the fourth-order moment is obtained using physical optics in the high frequency limit appropriate to near-vertical, specular backscatter. The solution is expressed as an asymptotic expansion valid to the second-order in Gaussian wave statistics and the first order in non-Gaussian wave statistics. The moment solution gives, to the first order in wave steepness, an intrinsic electromagnetic modulation spectrum that is proportional to the large wave directional slope spectrum evaluated in the azimuth of radar look. The harmonic distortion inherent to the specular scatter measurement of the sea slope spectrum is found to be small in the incidence angle range of 8 to 15 degrees.

Detailed consideration is given to the measurement signal-to-noise problems specific to SP and DF techniques. It is shown that with suitable pulse integration, typical satellite measurement signal-to-noise ratios of ca. 0 dB result for the narrowband DF technique and +20 dB for the SP technique. Thus, while satellite measurement feasibility with either technique is indicated, the SP technique possesses a distinct advantage in terms of measurement signal-to-noise and contrast ratios.

1. Introduction

Traveling by air over the ocean, have you ever noticed how clearly visible were the patterns of the ocean waves when direct sunlight illuminated the surface? I ask the question because I want to make the point that if these waves are visible to the naked eye, then surely they ought to be measurable by some remote sensing technique. In particular let us inquire if they cannot be measured by microwave radars which, as remote sensors, possess the distinct advantages of (a) providing their own source of illumination, (b) seeing through clouds and light rain and (c) being practically insensitive to the ionosphere. We will show that indeed microwave radars can measure the waves; moreover we show that the radars do not have to image the sea surface, if only statistical properties of the wave field are desired. The most useful statistical description of a random, homogeneous wave field is given by the directional wave height spectrum. In terms of the spatial properties of the wave field that are most easily observable from remote platforms, this is the two-dimensional, vector wave number spectrum of the two-dimensional height field.

Modern, numerical wave forecasting and analysis is based on wave spectral growth and propagation models that require as inputs initial sea state (i.e., directional wave spectra) and future wind field specifications. Owing to inevitable model and specification errors, the wave forecasts will be in error. Presently, there are no viable means, either *in-situ* or remote, of measuring directional ocean wave spectra in any kind of routine or global sense. If routine remote observations were to become available, we should be in a much better position to verify the wave forecasts currently being produced and to improve upon them, through both model improvement and improvement of the initial state specification.

We shall be considering observations of the sea surface in the case where the radar is pointing downward, away from the vertical, but not more than 15 degrees or so from the vertical. As is well known (Barrick, 1968a, 1974; Valenzuela, 1978), near-vertical microwave backscatter from the sea occurs by means of quasi-specular retroreflections from surface wave facets that are oriented normal to the radar line-of-sight. The backscatter can be described to various levels of approximation by

geometrical optics, physical optics, or higher-order high-frequency approximations (Jackson, 1974a); or alternatively, by composite surface theory (Brown, 1978). Basically though, the situation is one of specular reflection, and the radar backscatter problem can be compared to that of sun glint observation in the case where the sun is anti-parallel to the observer's line of sight.

I am concentrating here on small angle, specular backscatter for two reasons. One is that I believe that the physical mechanisms involved in the reflectivity modulation by the large waves are simpler than in the case of large-angle Bragg diffraction backscatter. At large angles there is, in addition to a purely geometrical tilting effect, a very strong sensitivity of the electromagnetic (em) modulation to the details of the hydrodynamic modulation of the centimetric Bragg-diffracting wavelets by the atmospheric and large ocean wave flow fields. While the hydrodynamic contribution to the large-angle reflectivity modulation has been treated theoretically (Alpers and Hasselmann, 1978; Valenzuela and Wright, 1979), theory is hard pressed to deal with the hydrodynamic complexities and actual field observations (Valenzuela and Wright, 1979; Wright et al., 1980). In the specular scatter regime, however, there is no special sensitivity to a particular small water wavelength. Rather, the entire ensemble of water waves is contributing to the population of specularly reflecting facets (excluding of course those wavelets smaller than the diffraction limit). For this large ensemble of waves, an assumption of Gaussian surface statistics seems to be a reasonable one, at least in the first order of approximation.

The second reason for concentrating on the near-vertical is a more practical one. It is desirable to make the nadir angle as small as possible in order that the radius of the azimuth scan circle on the ocean surface not exceed the distance over which the wave field can be expected to be homogeneous (cf. Fig. 1).

We have said that the radars need not actually image the surface to measure wave spectra. The idea behind the non-imaging radar measurement is simple: we let the broad em phase front on the surface (i.e., broad compared to the correlation scale of the waves) function to isolate or resolve plane Fourier surface contrast waves travelling in (or contrary to) the direction of radar look. The

principle is similar to that of Bragg scatter, which holds that backscatter occurs only from those water waves having wave vectors "matched" to the em propagation vector. Specifically, the water wave propagation vector $\underline{K}$ must lie in the plane of incidence and must have the magnitude

$$|\underline{K}| = 2\kappa \sin\theta$$

where κ is the em wave number and θ is the angle of incidence. To illustrate the principle we consider a simple tilting model of reflectivity variation in which the variation is directly proportional to the large wave slope component in the plane of incidence. See Fig. 2. Then if $\nabla\zeta$ is the large wave slope, the radar modulation spectrum will be proportional to the large wave directional slope spectrum evaluated in the azimuth of radar look, i.e.,

$$P_{mod}(\underline{K}) \propto \left(\frac{2\pi}{L}\right)^2 \left\langle \left| \int\int_{-L/2}^{L/2} \hat{\underline{\rho}} \cdot \nabla\zeta(\underline{x}) \, e^{-i\underline{K}\cdot\underline{x}} \, d\underline{x} \right|^2 \right\rangle \equiv |\underline{K}|^2 F(\underline{K})$$

where brackets $\langle \ldots \rangle$ denote ensemble average, $\hat{\underline{\rho}}$ is the unit horizontal vector, $\underline{K}/K$, and $F(\underline{K})$ is the spectrum of wave height.

The actual detection of the range-travelling surface contrast waves can be accomplished using either short pulse (SP) or dual frequency (DF) techniques. In the SP technique, very short pulses are used to resolve the surface wave structure in range. The fast-time or range modulation of the backscattered pulse caused by the spatial reflectivity variation can be detected by spectrum analysis of the backscattered signal envelope. (See Fig. 3.) The SP approach to possible satellite ocean wave measurement was apparently first suggested in a note by Tomiyasu (1971). Apart from the work of Jackson (1974b) and the present work, the SP approach has received no further consideration in the literature.

The DF approach, first proposed by Ruck *et al.* (1972) (and cf. also Ransone and Wright, 1972; Hasselmann, 1972) has received considerably more attention (Plant, 1977; Alpers and Hasselmann, 1978; Schuler, 1978; Plant and Schuler, 1980). The DF technique was originally proposed as – and is still generally understood to be – a narrowband technique. Quasi-monochromatic waveforms that entirely fill the antenna beam spot on the surface are transmitted at two closely separated

microwave frequencies. An harmonic surface contrast modulation is detected through the interaction of the em "beat wave" with the surface. Jackson (1974b) showed that the narrowband DF technique has a poor measurement SNR (signal-to-noise ratio) compared to the SP technique. The reason for the low SNR is that the contrast modulation spectrum is relatively broadband, having a bandwidth comparable to the bandwidth of the sea-slope spectrum (a bandwidth of the order of 50-100 percent of the peak frequency). Since the modulation spectrum $P_{mod}(\underline{K})$ is being detected only in a narrow spectral band of width $\Delta K \sim 2\pi/L_\rho$ where L_ρ is the range extent of illumination, the detected signal (the covariance of powers at the two frequencies) will be small compared to the background noise level (the variance of backscattered power at either frequency), i.e., the SNR $= P_{mod}(\underline{K}) \Delta K \ll 1$. Jackson (1974b) showed that this low SNR problem inherent to a narrowband DF measurement could be solved by using wideband signals – e.g., by using signals with bandwidths comparable to the sea-spectrum bandwidth. An illustration of a wideband DF radar system is given in Fig. 3. We note that the receiving system represented in Fig. 3b, consisting of a two channel receiver and cross-correlator, was described some years ago by Parzen and Shiren (1956). Parzen and Shiren considered both the SP and DF receiving systems from the viewpoint of detection theory. Independently of any particular transmitter, the SP and DF receiving systems were regarded simply as alternative systems for detecting a modulation on a noisy carrier signal. In their analysis, Parzen and Shiren assumed that the input to both detection systems was a weakly modulated Gaussian noise process. This is actually a realistic model of the sea-return process we are considering, and indeed a performance comparison of SP and DF systems can be made on the basis of such a model process (to be more specific, the surface impulse response can be modelled as a weakly modulated complex Gaussian process).

Alpers and Hasselmann (1978) (hereafter referred to as A-H) performed an extensive analysis of the DF technique in its original narrowband (continuous wave) context. Their analysis dealt with large-angle backscatter and included hydrodynamic modulation. Rather than using wideband signals to improve the DF SNR as suggested by Jackson (1974b), A-H instead introduced the idea of slow-time filtering the DF signal $D_{12}(t) = E_1(t)E_2^*(t)$ where E_1 and E_2 are the backscattered fields at the two frequencies. The idea is that the modulation signal component of $D_{12}(t)$ will appear as a strong

line in the comparatively broad Doppler spectrum of $D_{12}(t)$. A-H showed that by filtering $D_{12}(t)$ at the appropriate platform-motion-induced Doppler frequency, satellite SNRs typically of 0 dB could be obtained.

In this work, we apply the A-H filtering scheme to the SP technique as well as to the DF technique. In the SP technique, the slow-time filtering can be realized simply by integrating pulse returns in range bins (fast-time bins) that are adjusted so as to compensate for the apparent motion of the target ocean scene due to the motion of the platform. A schematic illustration of this kind of processing in a SP system is given in Fig. 4. (We remark that the integration, or filtering, is done to reduce the level of the random signal fluctuation arising from waveform coherency effects (Rayleigh fading).

Following, we present a frequency-domain analysis of the SP and DF systems illustrated in Fig. 3. This introduces the generalized fourth-order moment of the surface scattering transfer function. Using the scalar physical optics integral solution for the transfer function, we obtain, first, a time-independent, far-zone solution for the moment in the high-frequency limit appropriate to near-vertical backscatter (geometrical optics limit). We proceed then from the far-zone solution to the more complicated time-dependent Fresnel zone moment solution that is required for an analysis of the systems employing the A-H slow-time filtering. We conclude with an SNR analysis of SP and DF techniques which indicates the feasibility of measuring ocean wave directional spectra from low earth-orbiting satellites. The analysis shows that the processing gain achieved with the A-H filtering scheme is approximately the ratio of the microwave carrier frequency to the ocean-wave induced modulation frequency of interest. For X or Ku band radars, this ratio is on the order of +30 to +40 dB. With this processing gain, we arrive at typical satellite measurements SNRs of ca. -10 dB for the narrowband DF approach and ca. +20 dB for the SP approach.

2. Short-Pulse (SP) and Dual-Frequency (DF) Techniques

Figure 1 depicts a pencil beam of radiation incident on the sea surface. The antenna beam axis makes an angle θ to the vertical (z axis) and lies at an azimuth Φ relative to some (x_1, x_2) reference

axes in the horizontal plane. The unit vector $\hat{\rho} = (\cos\Phi, \sin\Phi)$ is defined as pointing along the azimuth ray, or in the direction of increasing surface range. The slant range from the radar to points on the surface $z = \zeta(\underline{x})$, $\underline{x} = (x_1, x_2)$, is denoted r, and the range to the center of the beam spot is denoted r_0. We shall be considering antenna beam widths typically of a few degrees and illuminated areas A_0 typically of several km in lateral and range extents.

We consider the backscatter of any finite duration but otherwise arbitrary transmitted waveform, $f(\tau)$. Here we use τ to denote "fast" signal time, i.e., that time having a scale commensurate with the pulse duration, or reciprocal pulse bandwidth (typical scale of microseconds). Fast time τ is to be distinguished from "slow" time t, which scales with the interpulse period or reciprocal Doppler bandwidth (typical scale of milliseconds). The incident field at the surface is given by the spherical wave $e^{inc}(\tau, \underline{x}) = G^{1/2}(\underline{x})f(\tau-r/c)/r$, where G is the antenna power pattern on the surface. The Fourier transform (FT) of the incident field is

$$E^{inc}(k, \underline{x}) = G^{1/2}(\underline{x})e^{-ikr}E_0(k) \tag{1a}$$

where $E_0(k)$ is the waveform FT at the surface,

$$E_0(k) = (c/2\pi)\int e^{-ikc\tau}[f(\tau)/r_0]\,d\tau \tag{1b}$$

where $k = \nu/c$ is the wave number, ν is the frequency and c the speed of light; and where in the denominator we have set $r = r_0$ since, for the few degree beamwidths and large ranges we are considering, r varies only very little over the beam spot. The backscattered field $e_s(\tau,t)$ is a duration-limited random process in fast time τ (the duration being determined by the round-trip travel time T_r of an impulse across the beam spot on the surface) and is assumed to be a stationary random process in slow time t. Stationarity in t follows if we assume that the radar is translating at a uniform velocity over a homogeneous sea. For simplicity, we will ignore the effect of discrete pulsing and sampling and treat $e_s(\tau,t)$ as a continuous process in t. Let the FT of e_s with respect to τ be denoted as $E_s(k,t)$. Then E_s is related to the incident wave form FT $E_0(k)$ as

$$E_s(k,t) = S(k,t)E_0(k) \tag{2}$$

where $S(k,t)$ is the surface scattering transfer function for backscatter at a frequency $\nu = kc$. In principle, $S(k,t)$ is the solution to the complex boundary value problem for a unit amplitude harmonic incident wave in the case where the scattering geometry is frozen at some time t. Note that we are treating S as a scalar quantity; this is permissible since there is only a very weak polarization dependence in the specular backscatter regime (cf. Jackson, 1974a). Also note that the look angle θ, Φ dependence is implicit in S.

A frequency-domain analysis of the SP and DF systems diagrammed in Fig. 3 is given in Appendix A. The SP and DF systems of Fig. 3 will, for convenience of identification, be referred to as "modulation noncoherent" systems, as they are insensitive to the phase of the signal modulation. In contradistinction, those systems which are sensitive to the phase of the modulation, such as the system of Figure 4, will be referred to as "modulation coherent." Since the idealized SP and DF systems double detect using square law detectors, their outputs will depend on fourth-order products of the surface transfer function $S(k,t)$. From Eqs. A2 and A8, it is seen that the ensemble average outputs of the SP and DF systems can be expressed in terms of different operations on the same "generalized" fourth-order statistical moment of $S(k,t)$, viz.,

$$M(k,k',\kappa) = \langle S(k)S^*(k-\kappa)S^*(k')S(k'-\kappa)\rangle \tag{3}$$

where $\langle \ldots \rangle$ denotes ensemble average and * complex conjugation. Note that in (3) we have omitted the explicit time dependence in $S(k,t)$. If the difference wave number Δk is defined as

$$\Delta k = k - k' \tag{3'}$$

then M can also be expressed as a function of Δk, $M = M(k, \Delta k, \kappa)$. In the following, we will be working under the assumption that the pulse bandwidths (or discrete difference frequencies) are not excessive; hence we require that

$$\kappa/k << 1 \text{ and } \Delta k/k << 1 \tag{3''}$$

In practice (3") will always be well satisfied; e.g., a 1 percent bandwidth would represent quite a large bandwidth.

3. Specular Scatter Solution for the Moment M(k,Δk,κ)

The physical optics (PO) integral solution for the transfer function can be written as (cf. Beckmann and Spizzichino, 1963; Weissman, 1973)

$$S(k,t) = \frac{ik\sec\theta}{2\pi r_0} \int G(\underline{x} - \underline{V}t) \exp\left[-i2kr(\underline{x},t)\right] d\underline{x} \tag{4}$$

where G is the illumination pattern; $\underline{V}$ is the platform velocity; $\underline{x} = (x_1, x_2)$ is the horizontal coordinate vector of surface points in a surface-fixed reference frame; $d\underline{x} = dx_1 dx_2$ is the element of horizontal area; and where the integration extends over the illuminated area. The origin of the coordinate system $\underline{x} = \underline{0}$ is taken to coincide with the center of the beam spot at $t = 0$. For small t, the Fresnel approximation to the phase is valid,

$$-2kr(\underline{x},t) \simeq -2kr_0 + 2k\cos\theta\zeta(\underline{x}) - 2k\sin\theta\,\hat{\underline{\rho}}\cdot(\underline{x} - \underline{V}t)$$

$$+ (k/r_0)\{|\underline{x} - \underline{V}t|^2 - \sin^2\theta\,[\hat{\underline{\rho}}\cdot(\underline{x} - \underline{V}t)]^2 + \zeta^2(\underline{x})\} \tag{5}$$

where again $\zeta(\underline{x})$ is the random wave height and $\hat{\underline{\rho}}$ is the unit vector in the horizontal pointing in the direction of increasing range. In the analysis of the modulation noncoherent systems of Fig. 3, we find that a far zone approximation to the phase is adequate; the quadratic Fresnel term in (5) can be dispensed with without sacrificing any of the essential physics of the problem. Thus, neglecting the Fresnel term (and ignoring the time dependence which is now trivial without the Fresnel term), we have for the far zone approximation to the PO integral:

$$S(k) = \frac{ike^{-i2kr_0}}{2\pi r_0\cos\theta} \int G(\underline{x})\exp\left\{i2k\left[\cos\theta\zeta(\underline{x}) - \sin\theta\,\hat{\underline{\rho}}\cdot\underline{x}\right]\right\} d\underline{x} \tag{6}$$

We calculate the fourth moment, Eq. (3), in the geometrical optics (GO) limit appropriate to near vertical, specular backscatter. The GO limit of the moment (3) can be calculated in a number of different ways according to various methods that can be found in the literature dealing with the second moment $\langle|S(k)|^2\rangle$ (average backscattered power). Of these methods, Barrick's (1968b) is the most direct. Other methods that start with the PO integral include those of Beckmann and

Spizzichino (1963) and Kodis (1966: cf. Weissman, 1973). Of course, it is possible to dispense with PO altogether and start *ab initio* with GO, e.g., using methods such as Lynch and Wagner's (1970). But, as we still have to account for phase, there is rea"y no advantage to be gained in using GO. Proceeding according to Barrick's (1968b) method, we substitute the PO integral (6) into (3). Writing the product as a four-fold integral, and interchanging ensemble average and integration operations, we have:

$$M(k,\Delta k,\kappa) = \left(\frac{k\sec\theta}{2\pi r_0}\right)^4 \int_{-\infty}^{\infty}\cdots\int G(\underline{x}^1)\ldots G(\underline{x}^4)$$

$$\cdot\left\langle\exp\{i2k\cos\theta[k(\zeta^1-\zeta^2-\zeta^3+\zeta^4)+\Delta k(\zeta^3-\zeta^4)\right.$$

$$\left.+\kappa(\zeta^2-\zeta^4)]\}\right\rangle\cdot\exp\{-2\sin\theta\,\hat{\varrho}\cdot[k(\underline{x}^1-\underline{x}^2$$

$$-\underline{x}^3+\underline{x}^4)+\Delta k(\underline{x}^3-\underline{x}^4)+\kappa(\underline{x}^2-\underline{x}^4)]\}\,d\underline{x}^1\ldots d\underline{x}^4 \qquad (7)$$

where we have approximated the product of the wave numbers $k(k-\kappa)\ldots$ by k^4 (which is permissible in view of (3″)), and where we have let $\zeta^1=\zeta(\underline{x}^1)$, etc. For large k (i.e., for large rms phase variation $2k\cos\theta<\zeta^2>^{1/2}$), it is apparent that appreciable contributions to the moment are made only in the neighborhoods of two sets of stationary points, *viz.*,

$$S_1:\ \underline{x}^1=\underline{x}^2,\ \underline{x}^3=\underline{x}^4$$

$$S_2:\ \underline{x}^1=\underline{x}^3,\ \underline{x}^2=\underline{x}^4 \qquad (8)$$

Except where $\underline{x}^1=\underline{x}^2=\underline{x}^3=\underline{x}^4$, the sets S_1 and S_2 are distinct and yield distinct contributions to the moment; i.e., $M=M_1+M_2$, where M_1 and M_2 respectively derive from integrations over the small volumes surrounding S_1 and S_2. Consider the integration over the volume containing S_1. Let

$$\underline{u}=2k\cos\theta(\underline{x}^1-\underline{x}^2)$$

$$\underline{v}=2k\cos\theta(\underline{x}^3-\underline{x}^4)$$

$$\underline{w}=\underline{x}^2-\underline{x}^4$$

$$\underline{x}=\underline{x}^4 \qquad (9a)$$

Now expand the height differences in the neighborhoods of the stationary points S_1 in a Taylor series,

$$2k\cos\theta(\zeta^1 - \zeta^2) = \nabla\zeta^2 \cdot \underline{u} + O(u^2/k)$$

$$2k\cos\theta(\zeta^3 - \zeta^4) = \nabla\zeta^4 \cdot \underline{v} + O(v^2/k) \qquad (9b)$$

where $\nabla \equiv (\partial/x_1, \partial/\partial x_2)$. Then the contribution M_1 to M for large k becomes

$$M_1 \sim (2r_0\cos^2\theta)^{-4} \int A(\underline{w}) \exp(-i2k\sin\theta \, \hat{\rho} \cdot \underline{w}) d\underline{w}$$

$$\times \left\{ (2\pi)^{-4} \int\int \left\langle \exp\left\{i[\nabla\zeta^2 \cdot \underline{u} - \nabla\zeta^4 \cdot \underline{v} \right.\right.\right.$$

$$+ 2\kappa\cos\theta(\zeta^2 - \zeta^4) + O((u^2 + v^2)/k) + O(\Delta kv/k)]\right\} \Big\rangle$$

$$\cdot \exp\left\{i[\tan\theta \, \hat{\rho} \cdot (\underline{u} - \underline{v}) + O(\Delta kv/k)]\right\} \, d\underline{u} \, d\underline{v} \Bigg\} \qquad (10)$$

where in (10) we have already taken the large k limit in the products of the gains, i.e., $G(\underline{x}^1)\dots G(\underline{x}^4) \sim G^2(\underline{x})G^2(\underline{x} + \underline{w})$, and where we have integrated over the remaining space variable $\underline{x}$, letting $A(\underline{w})$ represent the convolved two-way gain pattern,

$$A(\underline{w}) = \int_{-\infty}^{\infty} G^2(\underline{x})G^2(\underline{x} + \underline{w}) d\underline{x} \qquad (11)$$

(Since $\zeta(\underline{x})$ is a homogeneous random process in $\underline{x}$, the average $\langle \cdots \rangle$ is independent of the absolute position vector $\underline{x} = \underline{x}^4$, so that the $\underline{x}$ integration only effects the gain function.)

Now consider the limit of the factor in braces as $k \to \infty$. Let $\underline{\xi}$ denote the random six-vector,

$$\underline{\xi} = (\nabla\zeta^2, \nabla\zeta^4, \zeta^2, \zeta^4) \qquad (12a)$$

and let $\underline{t}$ denote the associated six-dimensional characteristic vector,

$$\underline{t} = (\underline{u}, -\underline{v}, 2\kappa\cos\theta, -2\kappa\cos\theta) \qquad (12b)$$

Then, the characteristic function of $\underline{\xi}$ is defined as

$$\psi_{\underline{\xi}}(\underline{t};\underline{w}) = \langle e^{i\underline{t}\cdot\underline{\xi}} \rangle = \int e^{i\underline{t}\cdot\underline{\xi}} \, p_{\underline{\xi}}(\underline{\xi};\underline{w}) d\underline{\xi} \qquad (13)$$

where $p_{\underline{\xi}}$ is the pdf (probability density function) of $\underline{\xi}$. Since $\zeta(\underline{x})$ (and hence $\underline{\xi}$) is a stationary process, the pdf and characteristic function depend only on the separation, or lag vector $\underline{w} = \underline{x}^3 - \underline{x}^4$.

From the definitions (12, 13) we have for M_1 in the high-frequency, GO limit, at least formally,

$$\lim_{k\to\infty} M_1 \equiv M_1(\kappa) = (2r_o\cos\theta)^{-4} \int A(\underline{w}) \exp(-i2\kappa\sin\theta\,\hat{\underline{\rho}}\cdot\underline{w})d\underline{w}$$

$$\times \left\{ (2\pi)^{-4} \int\int \psi_{\underline{\xi}}(\underline{t};\underline{w}) \exp[-i\tan\theta\,\hat{\underline{\rho}}\cdot(\underline{u}-\underline{v})]d\underline{u}\,d\underline{v} \right\} \tag{14}$$

Since M_1 in the large k limit is a function of κ only and the total moment $M = M_1 + M_2$, and since by the definition (3) M is symmetric with respect to a κ and Δk interchange, then we must have, in the limit,

$$\lim_{k\to\infty} M(k,\Delta k,\kappa) = M_1(\kappa) + M_1(\Delta k) \tag{15}$$

Note that the limit does not have to be taken in order that (15) hold true, at least approximately. The decomposition (15) will be valid in all cases provided that κ and Δk are small compared to k (condition (3″)).

If we define the surface wave vector

$$\underline{K} = 2\kappa\sin\theta\,\hat{\underline{\rho}} \tag{16}$$

and the specular slope vector

$$\underline{s} = \tan\theta\,\hat{\underline{\rho}} \tag{17}$$

Then (14) can be written somewhat more compactly as

$$M_1(\underline{K}) = (2r_o\cos^2\theta)^{-4} \int A(\underline{w})\exp(-i\underline{K}\cdot\underline{w})d\underline{w}$$

$$\times \left\{ (2\pi)^{-4} \int\int \psi_{\underline{\xi}}(\underline{t};\underline{w})\exp[-i\underline{s}\cdot(\underline{u}-\underline{v})]\,d\underline{u}\,d\underline{v} \right\} \tag{18}$$

where now the characteristic vector $\underline{t}$ has the components

$$\underline{t} = (\underline{u}, -\underline{v}, K\cot\theta, -K\cot\theta) \tag{19}$$

Let us write the solution (18) as

$$M_1(\underline{K}) = (2r_o\cos^2\theta)^{-4} \int_{-\infty}^{\infty} A(\underline{w})\,\Xi(K;\underline{w})\exp(-i\underline{K}\cdot\underline{w})d\underline{w} \tag{20}$$

where Ξ represents the factor in braces, *viz.*,

$$\Xi(K; \underline{w}) = (2\pi)^{-4} \iint_{-\infty}^{\infty} \psi_{\underline{t}}(\underline{u}, -\underline{y}, K\cot\theta, -K\cot\theta; \underline{w})$$

$$\cdot \exp[-i\underline{s}\cdot(\underline{u} - \underline{y})] \, d\underline{u} \, d\underline{y} \tag{21}$$

An alternative form of the solution may be obtained by using eq. (13) for $\psi_{\underline{t}}$ and integrating over $\underline{u}$ and $\underline{y}$:

$$\Xi(K; \underline{w}) = \iint_{-\infty}^{\infty} p_{\underline{t}}(\underline{s}, \underline{s}, \zeta^2, \zeta^4; \underline{w}) \exp[iK\cot\theta(\zeta^2 - \zeta^4)] \, d\zeta^2 \, d\zeta^4 \tag{22}$$

We shall find the form (21) more convenient to deal with.

Except in one particular (to which shortly), the above derivation is essentially identical to Barrick's (1968b) second-moment derivation. We have used Barrick's method because of the several approaches available it is the most direct and to the point. Yet, the reader may feel that the derivation lacks rigor; that certain steps require further justification. Rather than attempt this justification here, we offer instead in Appendix B an alternative, somewhat more rigorous derivation which sould, by analogy to the present derivation, justify it.

The peculiar feature of the fourth-moment solution alluded to (i.e., the feature of the fourth-moment solution that has no analogue in the second-moment problem) is this: the mathematical object claimed to be the solution does not exist. The joint pdf $p_{\underline{t}}$ is singular at the origin $\underline{w} = \underline{0}$, and the integral M_1 will — generally, it is supposed — be divergent. Consider the second moment of back-scattered monochromatic power, i.e., consider

$$\langle |S(k)|^4 \rangle = M(k, 0, 0) \sim 2M_1(\underline{0}) \tag{23}$$

Setting $\underline{K} = \underline{0}$ in (18) and (22), and in (22) integrating over ζ^1 and ζ^2, we have

$$M_1(\underline{0}) = (2r_0\cos^2\theta)^{-4} \int A(\underline{w}) \, p_{\nabla\zeta^2,\nabla\zeta^4}(\underline{s}, \underline{s}; \underline{w}) \, d\underline{w} \tag{24}$$

where $p_{\nabla\zeta^2,\nabla\zeta^4}$ is the joint pdf of slopes alone. For example, consider a one-dimensional scattering situation, where $\zeta(x)$ is the height profile and $\zeta_x(x)$ the slope. If $\zeta(x)$ is a stationary Gaussian process, then the joint pdf has a first-order singularity at the origin, i.e., as $w \to 0$ the joint pdf,

$$p_{\zeta_x^2,\zeta_x^4}(s, s; \underline{w}) \sim (2\pi)^{-\frac{1}{2}} p_{\zeta_x}(s) \cdot (g|w|)^{-1} \tag{25}$$

where $g = \langle \zeta_{xx}^2 \rangle$ is the rms curvature. Thus for Gaussian surfaces, the moment M_1 diverges logarithmically at the origin and consequently the variance of scattered power is infinite.

This singular behavior of the solution is a consequence of the point source approximation that is implicit in the PO integral formulation (4). The failure of the point source approximation can be understood in terms of the statistics of surface curvature. In the point source approximation ($r_0 \rightarrow \infty$), the power backscattered at a specular point is directly proportional to the product of the principal radii of curvature, or the same, the reciprocal of Gaussian curvature. Longuet-Higgins (1956) has derived the pdf of reciprocal Gaussian curvature g^{-1} for normally distributed surfaces and shown that the second moment of the distribution is infinite. We surmise that the unboundedness of the second moment of g^{-1} is not a property peculiar to Gaussian surfaces. Rather, we suppose that the variance of g^{-1} will be infinite for a large class of random surfaces. It can be shown that the singularity can be removed by including the finite dimensions of the source. When the finite size of the source is accounted for, the "singularity" at the origin is so reduced that its contribution to $M_1(\underline{Q})$ actually becomes quite small.

For reference, before concluding here, we write down the result for the second moment $\langle |S(k)|^2 \rangle$. From (4), using the same method we have used for the fourth-moment, we have for the second-moment in the high-frequency limit

$$\lim_{k \to \infty} \langle |S(k)|^2 \rangle = \left(\frac{A_o \sec^4\theta}{4 r_0^2} \right) p_{\nabla\zeta}(\underline{s}) \tag{26}$$

where the illuminated area $A_o = \int G^2 d\underline{x}$. In terms of the conventional backscatter cross-section,

$$\sigma_k^o \overset{\text{def}}{=} (4\pi r_0^2 / A_o) \langle |S(k)|^2 \rangle \tag{27}$$

we have

$$\sigma_\sim^o = \pi \sec^4\theta \, p_{\nabla\zeta}(\underline{s}) \tag{28}$$

In practice, it is found that the GO limiting form (28) provides a good fit to near-vertical microwave backscatter observations provided that some account is taken of the effects of diffraction for finite

k (Wentz, 1979). Diffraction can be accounted for by treating $p_{v\zeta}$ as though it were the pdf of slopes in a smoothed sea surface, in which waves smaller than the diffraction limit (e.g., capillary waves) have been removed by a spatial filter (cf. Brown, 1978). Thus, in (28), it is just as well to keep the finite frequency tag on σ°, as in practice, a k-dependent pdf is involved.

Following we will perform some calculations in which we assume a Gaussian pdf of orthogonal slopes,

$$p_{v\zeta}(\underline{s}) = (2\pi)^{-1}(\det \underline{\underline{m}})^{-\frac{1}{2}} \exp\left(-\frac{1}{2} m_{\alpha\beta}^{-1} s_\alpha s_\beta\right) \tag{29}$$

where $\underline{m}$ is the covariance matrix of orthogonal slope components,

$$\underline{\underline{m}} = (m_{\alpha\beta}) = \left\langle \frac{\partial\zeta}{\partial x_\alpha} \frac{\partial\zeta}{\partial x_\beta} \right\rangle, \quad \alpha = 1,2$$

and $m_{\alpha\beta}^{-1}$ are the elements of the inverse matrix. In (29) the Einstein summation convention is employed. A crude fitting of (28) with the Gaussian pdf to the 2.15 cm backscatter data of Jones *et al.* (1977) gives a 2.15 cm radar-effective total mean-square surface slope m_o^2 that is approximately a linear function of surface wind speed U,

$$\underset{\text{(Ku-band)}}{m_o^2} \simeq 0.0025\ U\ [\text{ms}^{-1}] + 0.01 \tag{30}$$

where the slope variance $m_o^2 = m_{\alpha\alpha}$. The eyeball-fitted result (30) is essentially the same as Wentz's (1979) more thorough analysis of the Jones *et al.* data. Eq. (30) gives radar-effective slope variances in the wind speed range 10 to 25 ms^{-1} that are approximately 60 percent of the optical values reported by Cox and Munk (1954). The Ku-band radar-effective slope-variance thus lies between the "clean" and "slick" surface observations of Cox and Munk (1954). Noteworthy is the agreement of the 60 percent figure, here derived from active radar cross-section data, with the percentage slope variance inferred from passive radiometric measurements using a GO model of emissivity (Wilheit, 1979).

4. Asymptotic Evaluation of M_1 (K)

We are considering wind-driven seas in which there is a continuous spectrum of roughness (i.e. wave height) from the scale of the dominant wave (~ 100 m) down to the scale of the diffraction limit (~ 0.1 m). If the incidence angle is not too large, there will always be a large population of scatterers (i.e. specularly reflecting wave facets) existing on scales smaller than the dominant ocean wavelength. The modulation of the backscatter by the large ocean wave (or spectral ensemble of large waves) can then be considered to be in the form of a small perturbation, and an asymptotic expansion of $\Xi(K; \underline{w})$ about $\underline{w} = \infty$ is appropriate. Let the large-wave steepness, or significant wave slope, be defined by $\delta_0 = K_0 \sigma$ where K_0 is the wave number of the dominant wave and σ is the rms wave height. Then the expansion should be accurate if δ_0 is small compared to the total rms slope, m_0. This will usually be the case. Thus if $\delta_0 = 0.05$ (a value characteristic of fully developed seas) and $m_0 = 0.19$ (wind speed of 10 ms^{-1} by (30)), then $\delta_0/m_0 = 0.26$.

M_1 (K) (eq. 20) is expanded by first expanding $\Xi(K; \underline{w})$ (as given by eq. 21) and then term-by-term Fourier transforming with respect to $\underline{w}$. Ξ is expanded according to Longuet-Higgins' (1963) method for generating the non-Gaussian pdf's of variables in a non-linear Stokesian sea. Indeed, we have chosen the form (21) for Ξ in order that we could parallel Longuet-Higgins' (1963) development and so lay the foundation for a theoretical model of M_1 (K) capable of entertaining non-Gaussian wave statistics in a rational manner.

As can be seen from (13) the coefficients in a Taylor series expansion of the characteristic function correspond to the moments of the distribution, i.e., if

$$\psi_{\underline{t}}(\underline{t}; \underline{w}) = 1 + \frac{i}{1!} \mu_i^{(1)} t_i + \frac{i^2}{2!} \mu_{ij}^{(2)} t_i t_j + \dots \tag{31}$$

then the μ coefficient of order n is the n-th order moment,

$$\mu_{i_1 \dots i_n}^{(n)}(\underline{w}) = \int (\xi_{i_1} \dots \xi_{i_n}) \, p_{\xi}(\underline{\xi}; \underline{w}) \, d\underline{\xi} \tag{32}$$

The cumulants of the distribution, by definition, correspond to the c coefficients in the expansion of

$$C_{\underline{\xi}}(\underline{t}; \underline{w}) = \ell n \, \psi_{\underline{\xi}}(\underline{t}; \underline{w})$$

$$= \frac{i}{1!} c_i^{(1)} t_i + \frac{i^2}{2!} c_{ij}^{(2)} t_i t_j + \dots \qquad (33)$$

Longuet-Higgins (1963) shows how, in general, it is easier to calculate the cumulants (as opposed to the moments) from the non-linear, Eulerian water wave equations. Further, an advantage in working with the cumulants is that if $\underline{\xi}$ is nearly normally distributed, then the third and higher-order terms in the C series will be small. (This is so since for $\underline{\xi}$ exactly normal, C is given exactly by the first two terms of the expansion (33).) Considerable simplification of the problem is possible if we restrict our attention to statistics of the third-order or less. Thus, since $\underline{\xi}$ (cf. eq. 12a) has zero mean, $c^{(1)} = \mu^{(1)} = 0$, it follows that the second and third order moments and cumulants are identical, as can be verified by a term-by-term comparison of (31) and the expansion of $\psi_{\underline{\xi}} = \exp(C_{\underline{\xi}})$. Thus, if we restrict ourselves to third-order statistics, $\psi_{\underline{\xi}}$ can be approximated by

$$\psi_{\underline{\xi}} = \exp(C_{\underline{\xi}}) \sim \exp\left[-\frac{1}{2} \mu_{ij}^{(2)}(\underline{w}) t_i t_j\right] \cdot$$

$$\times \left\{1 + \frac{i^3}{3!} \mu_{ijk}^{(3)}(\underline{w}) t_i t_j t_k\right\} \qquad (34)$$

All elements of the covariance matrix $\mu_{ij}^{(2)} = \langle \xi_i \xi_j \rangle$ can be expressed in terms of the wave height covariance function $R(\underline{w})$,

$$R(\underline{w}) \stackrel{\text{def.}}{=} \langle \zeta^2 \zeta^4 \rangle = \langle \zeta(\underline{x} + \underline{w}) \zeta(\underline{x}) \rangle \qquad (35)$$

or various derivatives thereof, as can be verified, for example, using methods outlined in Papoulis (1965, p 314 ff):

$$\underline{\mu}^{(2)} = \begin{bmatrix} m_{\alpha\beta} & -R_{,\alpha\beta} & 0 & -R_{,\alpha} \\ & m_{\alpha\beta} & R_{,\alpha} & 0 \\ S_{ymmetric} & & \sigma^2 & R \\ & & & \sigma^2 \end{bmatrix} \qquad (36)$$

where we have defined $\sigma^2 = R(\underline{0})$, $R_{,\alpha} = \partial R(\underline{w})/\partial w_\alpha$ etc. and $m_{\alpha\beta} = -R_{,\alpha\beta}(\underline{0})$, and where α and β range from 1 to 2.

Let $\underline{\mu}^{(2)} = {}^d\underline{\mu}^{(2)} + {}^o\underline{\mu}^{(2)}$ where d and o denote the diagonal and off-diagonal blocks of $\underline{\mu}^{(2)}$. Since ${}^d\underline{\mu}^{(2)} = 0(m_0^2)$ and ${}^o\underline{\mu}^{(2)} = 0(\delta_0^2)$ for $\underline{w}$ removed from the origin, i.e. on the order of wavelength, we can then expand (34) for small ${}^o\underline{\mu}^{(2)}$,

$$\psi_{\underline{\xi}} \sim \exp\left(-\frac{1}{2}{}^d\mu_{ij}^{(2)}t_it_j\right) \times \left[1 - \frac{1}{2}{}^o\mu_{ij}^{(2)}t_it_j\right.$$

$$\left. - \frac{i}{6}\mu_{ijk}^{(3)}t_it_jt_k + \frac{1}{8}{}^o\mu_{ij}^{(2)}{}^o\mu_{kl}^{(2)}t_it_jt_kt_l \cdots\right] \tag{37}$$

where ${}^o\underline{\mu}^{(2)}$ and $\underline{\mu}^{(3)}$ are functions of $\underline{w}$, but ${}^d\underline{\mu}^{(2)}$ is not. Similarly to (36) we expect that the elements of $\underline{\mu}^{(3)}$ are all derivable from a knowledge of the third-order mean lagged products of surface height $Q(\underline{r}, \underline{s}) = \langle \zeta(\underline{x} + \underline{r})\zeta(\underline{x} + \underline{s})\zeta(\underline{x})\rangle$. Thus, the FT of $\underline{\mu}^{(3)}(\underline{w})$ should be expressible as various operations on the bispectrum, the FT of $Q(\underline{r}, \underline{s})$ (Hasselmann *et al.*, (1963). In principle, the bispectrum (and hence the elements of $\underline{\mu}^{(3)}$ and the FT of $\underline{\mu}^{(3)}$) can be derived from the height of spectrum $F(\underline{K}) = FT\{R(\underline{w})\}$ using a second-order Stokes type expansion of the nonlinear equations for free gravity waves according to the theories of Hasselmann *et al.* (1963) and Longuet-Higgins (1963).

We are thus proposing here that the appropriate model for the near-vertical wave-spectrum measurement problem is one that (a) models scattering according to GO and (b) models the sea-surface according to the Longuet-Higgins (1963) and Hasselmann *et al.* (1963) theories. That this is a realistic model for near vertical backscatter is indicated, for one, by the success of such a model in predicting the average impulse response of the sea surface to 3 cm radiation at vertical incidence (Jackson, 1979). Moreover, regarding the appropriateness of the GO approximation: if there is reason to suppose that GO is a good approximation in the average impulse response problem, then there is even more reason to suppose that GO is a good approximation in the present problem, i.e. that of modelling the spectrum of the impulse response. This is because in the present problem we are only interested in the variation of the backscatter over the large wave profile, and not in the

absolute power level. Thus, while the diffraction component may be small compared to the GO component (cf. Brown, 1978), the variation of the diffraction component will be smaller still compared to the GO component. This is because the diffracted fields are very diffuse, and can therefore contribute only negligibly to the modulation *via* the geometrical tilting mechanism.

We shall be neglecting the non-Gaussian terms in $\mu^{(3)}$, although there is no reason to suppose *a priori* that the $\mu^{(3)}$ terms are negligible compared to the second-order terms in $^o\mu^{(2)}$. Thus, for example, consider small values of $\tan\theta/m_o$. Then the $^o\mu^{(2)}$ terms such as $R(\underline{w})K^2\cot^2\theta$ predominate. Thus the linear term is $0(K^2\sigma^2\cot^2\theta) = 0(\delta_o^2\cot^2\theta)$ and the second order $^o\mu^{(2)}$ term is $0(\delta_o^4\cot^4\theta)$. The corresponding $\mu^{(3)}$ term will be $0(\lambda\sigma^3K^3\cot^3\theta) = 0(\lambda\delta_o^3\cot^3\theta)$ where $\lambda = \langle\zeta^3\rangle/\sigma^3$ is the height skewness coefficient. In general, λ and δ_o are proportional to each other (Huang, 1980; Jackson, 1979). From Longuet-Higgins' (1963) theory, if one assumes a Phillips spectral form, one gets $\lambda = 4\delta_o$. This relationship follows from Jackson (1979) if an apparent error of a factor of two in the second-order height profile ζ_2 is corrected for; i.e. if $\zeta_2 \leftarrow \zeta_2 + 2$ (D. E. Barrick, personal communication, 1980). The ratio of $\mu^{(3)}$ terms to second-order $^o\mu^{(2)}$ terms is then of the order of $\lambda/\delta_o\cot\theta = 4\tan\theta = 0.71$ for $\theta = 10°$. Hence, *a priori*, the neglect of the $\mu^{(3)}$ terms is not justified.

Proceeding nevertheless with a Gaussian surface model, using (36) and (19) (for the definition of $\underline{t}$), we have

$$\psi_{\underline{t}} \sim \psi_{\nabla\zeta}(\underline{u}) \psi_{\nabla\zeta}(-\underline{v}) \exp[-(K\sigma\cot\theta)^2]$$

$$\times \left\{ 1 + (K\cot\theta)^2 R + K\cot\theta R_{,a}(u_a - v_a) \right.$$

$$\left. -R_{,a\beta}u_a v_\beta + \text{second-order terms in } ^o\mu^{(2)} \right\} \tag{38}$$

where $\psi_{\nabla\zeta}(\underline{u}) = \exp(-\tfrac{1}{2}m_{a\beta}u_a u_\beta)$. The second-order terms are carried in Appendix C. Now making use of the identities,

$$p_{\nabla\zeta}(\underline{s}) = \frac{1}{(2\pi)^2} \int \psi_{\nabla\zeta}(\underline{u})e^{-i\underline{s}\cdot\underline{u}} d\underline{u}$$

$$\frac{\partial p_{\nabla\zeta}}{\partial s_a} = \frac{i}{(2\pi)^2} \int u_a \psi_{\nabla\zeta}(\underline{u})e^{-i\underline{s}\cdot\underline{u}} d\underline{u} \tag{39}$$

and so forth, we have for Ξ (eq. 21)

$$
\Xi \sim p_{\nabla\zeta}^2(\underline{s}) \exp[-(K\sigma\cot\theta)^2] \cdot \Bigg\{ 1 +
$$

$$
+ (K\cot\theta)^2\, R + 2iK\cot\theta\, \frac{p_{,a}}{p}\, R_{,a}
$$

$$
- \frac{p_{,a}\, p_{,\beta}}{p^2}\, R_{,a\beta} + \text{second-order terms in } {}^o\underline{\mu}^{(2)} \Bigg\} \qquad (40)
$$

where for short in the series part of (40) we have let $p \equiv p_{\nabla\zeta}(\underline{s})$ and $p_{,a} \equiv \partial p/\partial s_a$, etc. The second-order terms are carried in Appendix C.

The moment $M_1\,(\underline{K})$ as given by (20) is the FT of Ξ as seen through the lag window $A(\underline{w})$. If $A(\underline{w})$ is broad compared to the correlation scale of the waves (as will always be the case in satellite measurements), then the effect of the finite window on the modulation spectrum can be igonred and we can write M_1 as

$$
M_1(\underline{K}) = (\pi/2r_o^2\cos^4\theta)^2\, p_{\nabla\zeta}^2(\underline{s})\exp[-(K\sigma\cot\theta)^2]
$$

$$
\times \Big[\text{FT}\{A(\underline{w})\} + A(\underline{0})\cdot \text{FT}\{\text{linear} + \text{higher-order terms in (40)}\}\Big] \qquad (41)
$$

where the two-dimensional Fourier transform,

$$
\text{FT}\{\ldots\} \overset{\text{def.}}{=} \frac{1}{(2\pi)^2}\int\{\ldots\}\, e^{-i\underline{K}\cdot\underline{w}}\, d\underline{w} \qquad (42)
$$

Let the reference axes x_1 and x_2 be fixed in the antenna beam; that is let x_1 be the surface range coordinate, parallel to $\hat{\rho}$ and $\underline{K}$, and let x_2 be the orthogonal azimuthal coordinate. Assume a Gaussian gain pattern,

$$
G(\underline{x}) = \exp\left[-\frac{1}{2}(x_1/L_\rho)^2 - \frac{1}{2}(x_2/L_\phi)^2\right] \qquad (43)
$$

then (using (11) for $A(\underline{w})$),

$$
\text{FT}\{A(\underline{w})\} = (2\pi)^{-2}\int\int A(w_1,w_2)\exp(-iKw_1)dw_1 dw_2
$$

$$
= (A_o/2)\exp\left[-\frac{1}{2}(KL_\rho)^2\right] \qquad (44)
$$

Then, making use of the second-moment result (25), noting that $A(\underline{0}) = A_0/2 = \pi L_\rho L_\phi/2$, we write (41) in the form

$$M_1(\underline{K}) = \frac{\sqrt{2\pi}}{L_\rho} \ [\langle|S(k)|^2\rangle]^2 \left\{ \frac{L_\rho}{\sqrt{2\pi}} e^{-\frac{1}{2}(KL_\rho)^2} + P_{mod}(\underline{K}) \right\} \qquad (45)$$

where the modulation spectrum, or spectrum of the impulse response, is

$$P_{mod}(\underline{K}) = (\sqrt{2\pi}/L_\phi) \exp[-(K\sigma\cot\theta)^2] \cdot FT\{\text{linear} + \text{higher-order terms in (40)}\} \qquad (46)$$

The directional height spectrum is defined by

$$F(\underline{K}) \overset{def.}{=} FT\{R(\underline{w})\} \qquad (47)$$

Then, since $FT\{R_{,a}\} = iK_a F(\underline{K})$ and $FT\{R_{,a\beta}\} = -K_a K_\beta F(\underline{K})$, the expansion for P_{mod} becomes

$$P_{mod}(\underline{K}) = \frac{\sqrt{2\pi}}{L_\phi} e^{-(K\sigma\cot\theta)^2} \cdot \left\{ \left[\cot^2\theta - 2\cot\theta \ \frac{p_{,a}}{p} \cdot \frac{K_a}{K} \right. \right.$$

$$\left. \left. + \frac{p_{,a}p_{,\beta}}{p^2} \cdot \frac{K_a K_\beta}{K^2} \right] K^2 F(\underline{K}) + \dots \right\} \qquad (48)$$

or

$$P_{mod}(\underline{K}) = \frac{\sqrt{2\pi}}{L_\phi} e^{-(K\sigma\cot\theta)^2} \cdot \left\{ \left(\cot\theta - \frac{\partial \ln p}{\partial s} \right)^2 K^2 F(\underline{K}) + \dots \right\} \qquad (49)$$

where $\partial\ln p/\partial s \equiv (K_a/K)\cdot(p_{,a}/p) \equiv \hat{\rho} \cdot \nabla_s p$. The second-order term in the expansion of P_{mod} is given in Appendix C.

Some features of the solution are noted. If the exponential factor (the square of ψ_ξ) is neglected (which neglect is consistent with the neglect of the second-order terms) then the linearized solution (49) yields the same result as the simple tilting model (Fig. 2). The dimensional proportionality factor L_ϕ^{-1} relating $P_{mod}(\underline{K}) \triangleq$ m to $K^2F(\underline{K}) \triangleq$ m^2 is the reciprocal of the azimuthal beam spot dimension. An L_ϕ^{-1} dependence will exist whenever L_ϕ exceeds the lateral correlation length scale (e.g. crest length) of the surface waves. Large L_ϕ means small signal. This loss of modulation signal power with increasing L_ϕ can be thought of as the price paid for high directional resolution: of the ensemble of Fourier component surface waves contributing to a total modulation

power, the radar is isolating only a small subset that are travelling in a small direction band. The L_ϕ^{-1} dependence can also be interpreted as follows: in a real short-crested sea, the waves are running out-of-step. Hence, modulation signal power adds noncoherently across the beamwidth resulting in an $L_\phi^{1/2}$ dependence. The total signal power on the other hand adds directly as L_ϕ. Hence the relative modulation power goes as $L_\phi^{-1/2}$, and the spectrum of power as L_ϕ^{-1}.

To gain some feel for the effect of the second-order terms, sample calculations are carried out for a simplified two-dimensional scattering situation using eqs. 49 and C5 of Appendix C. The results shown in Fig. 5 indicate that there is a fairly good measurement fidelity to the wave slope spectrum in the incidence angle range 8° to 15° for wind speeds > 5 ms^{-1} and significant wave slopes $\delta_0 < 0.1$.

5. SNR Analysis: The Modulation Noncoherent Case

Narrowband Dual-Frequency (DF) Technique

The appropriate signal-to-noise ratio (SNR) in the narrowband DF technique is the DF correlation coefficient (cf. Barrick, 1972; Plant, 1977). Thus, from (3), (15), and (45), we have

$$SNR \overset{def.}{=} \frac{M(k,\kappa,0)}{[\langle |S(k)|^2 \rangle]^2} - 1$$

$$= (\sqrt{2\pi}/L_\rho) \, P_{mod}(\underline{K}) \tag{50}$$

In (50), note that P_{mod} is the one-sided spectrum, i.e., we have let $P_{mod} \leftarrow 2P_{mod}$. Here, and in the SNR calculations that follow, we use only the linear part of P_{mod} with the exponential set equal to unity. (This assumes that $\delta_0\cot\theta << 1$, and is consistent with the neglect of the second-order terms.) Let the one-sided spectrum $F(\underline{K})$ be given by the Phillips spectral form with a $\cos^4 \Phi$ spreading factor,

$$F(\underline{K}) = (0.005)(8/3\pi)\cos^4\Phi K^{-4}, \quad \begin{cases} K > K_o \sim g/U^2 \\ |\Phi| < \pi/2 \\ 0 \text{ otherwise} \end{cases} \tag{51}$$

This spectrum defines a sea with a steepness $\delta_0 = K_o\sigma = K_o[\int F(\underline{K})d\underline{K}]^{1/2} = 0.05$. For upwind (up-wave) looks $\Phi = 0$, and $F(\underline{K}) = 0.0042K^{-4}$. From (28) with $\underline{s} = \tan\theta(1,0)$, we have $\partial \ln p/\partial s =$

$-\tan\theta/m_{10}$; hence,

$$P_{mod}(\underline{K}) \simeq (\sqrt{2\pi}/L_\phi)\,(\cot\theta + \tan\theta/m_{10})^2\,(0.0042)K^{-2} \tag{52}$$

Let $K = K_0 = 2\pi/200$ m, and corresponding to which, $U \simeq \sqrt{g/K_0} = 18$ ms^{-1}. If we use the Cox and Munk (1955) upwind/crosswind slope variance ratio $m_{01} \simeq .66\,m_{10}$, then $m_{10} \simeq m_0^2/1.66$. From (30), we have $m_0^2 \simeq 0.055$ and so $m_{10} \simeq 0.033$. Let $\theta = 12.5°$ and $L_\phi = 2.5$ km; then

$$P_{mod} \simeq (10^{-3}\text{ m}^{-1})\,(4.5 + 6.7)^2\,(4.3\text{ m}^2) = 0.54\text{ m} \tag{53}$$

If $L_\rho = 5$ km, then from (50), the SNR $= -36$ dB. In addition to the SNR, defined here as the ratio of the modulation signal spectrum to the square of the average power (equals the self-clutter, or random power fluctuation variance), we need a figure to express the signal strength relative to the average backscattered power. Call this figure the contrast ratio,

$$CR \overset{\text{def.}}{=} [P_{mod}(\underline{K})\,\Delta K]^{1/2} = (SNR)^{1/2} = 1.6\% \tag{54}$$

where the last follows since $\Delta K = \sqrt{2\pi}/L_\rho$.

Short Pulse (SP) Technique

The frequency-domain analysis of the SP system of Fig. 3a is carried out in Appendix A. In the transformation between frequency and wave number domains, we have the identities $\nu = kc$, $\omega = \kappa c$, and $\Delta\nu = \Delta kc$. Since $K = 2\kappa\sin\theta$, etc., the moment result, eqs. (15) and (45) becomes in the frequency domain

$$M(\nu,\Delta\nu,\omega) = M_1(\nu,\omega) + M_1(\nu,\Delta\nu) \tag{55}$$

where

$$M_1 = (\sqrt{2\pi}/T_r)[(|S(\nu)|^2)]^2\{\delta(\omega) + P_{mod}(\omega,\Phi)\} \tag{56}$$

and where $T_r \equiv (2L_\rho/c)\sin\theta$ and where for large T_r we have let

$$\delta(\omega) \sim (T_r/\sqrt{2\pi})\exp\left[-\frac{1}{2}(\omega T_r)^2\right]$$

where $\delta(\omega)$ is the Dirac delta function.

The backscatter of a short pulse (i.e. "short" compared to the ocean wavelength) consists of a weak modulation $m(\tau)$ riding in a broadband, exponential "self-clutter" process $w_c(\tau)$ of bandwidth equal to the pulse bandwidth β_p. (The exponential statistics of $w_c(\tau)$ follow from an assumption of normal statistics for the unmodulated complex field.) Thus, the backscatter power is of the form $p(\tau) = \bar{p}\,[1 + m(\tau)]\,w_c(\tau)$. Using either this simple time-domain model, or using the moment analysis results of Appendix A, one finds that the spectrum of $p(\tau)$ has the form (e.g., assuming a Gaussian-shaped pulse):

$$P(\omega) \propto \frac{\sqrt{2\pi}}{T_r} [\langle|S(\nu)|^2\rangle]^2 \, e^{-\frac{1}{2}(\omega/\beta_p)^2} \left\{ \delta(\omega) + \frac{1}{\sqrt{2\pi}\beta_p} + P_{mod}(\omega,\Phi) \right\} \qquad (57)$$

where the approximation is valid for small modulation, i.e. for $\int P_{mod}(\Delta\nu)\Delta\nu \ll 1$. Eq. (57) is sketched in Figure 6.

Note that, if we let $\beta_p \to \infty$, then the transmitted pulse becomes an impulse. Thus P_{mod} is just the normalized spectrum of the surface impulse response. The SNR appropriate to the SP technique is the ratio of the signal spectrum to the self-clutter noise spectrum, i.e. the SNR $= \sqrt{2\pi}\,\beta_p P_{mod}$. Now, some or all of β_p may be used for range resolution. A minimum pulse bandwidth is required to achieve a desired range resolution (e.g. 25 m on the surface). Bandwidth in excess of this minimum serves to reduce the level of the self-clutter spectrum. If we define an equivalent range resolution cell Δ_ρ such that if all the bandwidth were utilized for range resolution, i.e. $\Delta_\rho = c/2\beta_p\sin\theta$, then we can express the SNR in a form similar to (50). If we take as an example $\Delta\rho = 5$ m, then (again using (53) for the estimate of P_{mod})

$$SNR = (\sqrt{2\pi}/\Delta\rho)\,P_{mod}(\underline{K}) = -6 \text{ dB} \qquad (58)$$

which is 30 dB above the narrowband DF SNR, i.e. grater by the factor $L_\rho/\Delta\rho$. The contrast ratio is defined as the ratio of the rms signal level to the dc level; from (52) we have

$$CR = \left[\int_{K_o}^{\infty} P_{mod}(\underline{K})dK \right]^{\frac{1}{2}} = 13\% \qquad (59)$$

As the SNR can always be improved by pulse integration (as we shall shortly show), the CR could turn out to be the more important figure in design considerations. The 13 percent figure is quite good; what is more, the CR will still be quite good for shorter waves since $CR \propto K_0^{-\frac{1}{2}}$. Thus, e.g., for a fully developed ($\delta_0 = 0.05$) sea wave of 50 m in length, the CR is reduced by only a factor of two from the 13 percent CR of the 200 m water wave we have used as an example.

Wideband DF Technique

The wideband DF technique can employ a variety of waveforms including SP waveforms. (Thus, if we transmit pulses shorter than the dominant waves then, necessarily, all the required difference frequencies are carried by the pulse.) If the transmitted waveform FT is, for example, assumed to be constant over the bandpasses of the filters H_i and H_j of Figure 3b then, as shown in Appendix A, the strength of the DF signal at the output of the correlator will be governed by the combined bandwidth $\beta_{a ij}$ of the H_i and H_j analyzing filters in each channel (cf. Figure 3b). Owing to the action of the dc blocking filters and the fact that the self-clutter fluctuation power is uncorrelated between frequency bands $\Delta \nu \geq 2\pi/T_r$, the expected value of the output of this DF system will contain neither dc nor self-clutter components.

So, what is the appropriate SNR for this system? And how should this system's performance be compared to the SP system? Clearly, we have to look at the detection problem more carefully. Parzen and Shiren (1956) went some distance toward this by establishing a detection criterion for the SP system. Unfortunately, they stopped short of a like analysis of the DF system. Lacking a rigorous analysis by Parzen and Shiren, we will do with some back-of-the-envelope calculations. Assume that the signal levels are within the dynamic range and resolution capabilities of the instruments. Assume further that we can ignore the sampling variability in the estimate of P_{mod} compared to the variability in the self-clutter spectrum. Then, successful measurement depends only on the strength of the signal relative to the self-clutter fluctuation levels about their expected values. Consider the SP system. The signal at a frequency ω_i appearing through a finite analysis window of bandwidth β_{ai} is $\beta_{ai} P_{mod}(\omega_i)$. The mean noise level is $\beta_{ai}/\sqrt{2\pi}\beta_p$. The noise standard deviation in

a measurement of total time-bandwidth product $TBP = N_p T_r \beta_{ai}/2\pi$ where N_p is the total number of independent pulses, is $(\sqrt{2\pi}\beta_p)^{-1} (TBP)^{-1/2}$. Hence, if we define the detectability D^* as the ratio of the signal to the noise standard deviation, then

$$D^*_{SP} = (N_p \beta_{ai} T_r)^{1/2} \beta_p P_{mod}(\omega_i, \Phi) \tag{60}$$

In the DF system, the signal out is proportional to $\beta_{aij} P_{mod}(\Delta\nu_{ij})$. Assume that the mean square fluctuation of cross-correlated power as a percentage of the product of mean channel powers is simply $TBP^{-1/2}$ where $TBP = N_p \beta_{aij} T_r/2\pi$. If this assumption is correct then the D^* for the DF system is

$$D^*_{DF} = (N_p T_r)^{1/2} \beta^{3/2}_{aij} P_{mod}(\Delta\nu_{ij}, \Phi) \tag{61}$$

If the DF analysis bandwidth β_{aij} is opened wide (i.e., made comparable to the $\Delta\nu_{ij}$), then D^*_{DF} is comparable to the D^*_{SP}. Any further analysis of SP and DF techniques must consider thermal noise, antenna gain and other tradeoffs. This is beyond the scope of the present work and is, after all, academic, considering that the SNR can be improved immediately by making the detection coherent with respect to the modulation signal.

6. A-H Filtering: The Modulation Coherent Case

Alpers and Hasselmann (1978) showed how by filtering the complex DF signal

$$D(\kappa, t) = S(k, t) S^*(k - \kappa, t) \tag{62}$$

at the appropriate Doppler frequency $\Omega = \underline{K} \cdot \underline{V}$, a dramatic increase in the narrowband DF SNR could be had. We show how, if the same type of processing is applied to an SP system, the same dramatic increase in SNR results. As the narrowband DF results follow immediately from the more general moment results in the analysis of the wideband systems, we proceed directly with the wideband analysis problem.

Consider the SP system of Figure 4. The output of the square-law detector is $p(\tau, t) = |e_s(\tau, t)|^2$. The FT of p with respect to fast time is denoted $P(\omega, t)$,

$$P(\omega, t) = \int_{-\infty}^{\infty} E_s(\nu, t) E^*_s(\nu - \omega, t) d\nu \tag{63}$$

where by (2) $E_s(\nu, t) = S(\nu, t)E_o(\nu)$. The pulse spectrum is defined as $P(\omega) = \langle |P(\omega, t)|^2 \rangle$. The simple filter in Figure 4 functions to integrate pulse returns in surface-fixed range bins. The output of the filter after an integration time T_{int} is

$$\widetilde{p}(\tau) = \frac{1}{T_{int}} \int_0^{T_{int}} p(\tau + \dot{\tau}t, t)\, dt \tag{64}$$

where $\dot{\tau} = 2\dot{r}/c$. The spectrum of the filtered pulse return is $\widetilde{P}(\omega) = \langle |\widetilde{P}(\omega, t)|^2 \rangle$ where $\widetilde{P}(\omega)$ is the FT of $\widetilde{p}(\tau)$. The spectrum of the filtered pulse return can be expressed as

$$\widetilde{P}(\omega) = \int_{-\infty}^{\infty} W(\Omega - \underline{K} \cdot \underline{V})\, P(\omega, \Omega)\, d\Omega \tag{65}$$

where the filter window $W(\Omega)$

$$W(\Omega) = \left[\frac{\sin(\Omega T_{int}/2)}{(\Omega T_{int}/2)} \right]^2 \tag{66}$$

and $P(\omega, \Omega)$ is the post-detection pulse-Doppler spectrum defined by

$$P(\omega, \Omega) = \frac{1}{2\pi} \int_{-\infty}^{\infty} \langle P(\omega, t)\, P^*(\omega, t + \Delta t) \rangle e^{i\Omega \Delta t}\, d\Delta t \tag{67}$$

The Doppler frequency $\Omega = \underline{K} \cdot \underline{V} = -\omega\dot{\tau}$. If $\Phi = 0$ coincides with the velocity vector as in Figure 1, then

$$\Omega = \underline{K} \cdot \underline{V} = KV\cos\Phi \tag{68}$$

If the generalized moment is defined as

$$M(\nu, \nu', \omega; \Delta t) = \langle S(\nu, t)\, S^*(\nu - \omega, t)\, S^*(\nu', t + \Delta t)\, S(\nu' - \omega, t + \Delta t) \rangle \tag{69}$$

and the FT of M with respect to Δt,

$$N(\nu, \nu', \omega; \Omega) = \frac{1}{2\pi} \int_{-\infty}^{\infty} M(\nu, \nu', \omega; \Delta t)\, e^{i\Omega\Delta t}\, d\Delta t \tag{70}$$

then

$$P(\omega,\Omega) = \iint\limits_{-\infty}^{\infty} N(\nu,\nu',\omega;\Omega) \, E_0(\nu) \, E_0^*(\nu-\omega) \, E_0^*(\nu') \, E_0(\nu'-\omega) \, d\nu \, d\nu' \qquad (71)$$

Now let us again equate the fast frequencies ν, ν', and ω with the wavenumbers k, k', and κ, (by $\nu = kc$, etc.), so that in terms of wavenumber $M = M(k, k', \kappa) \equiv M(k, \Delta k, \kappa)$. We calculate M with $S(k,t)$ given by PO integral solution (4) in the Fresnel approximation to the phase (5), where we neglect the term in height, $k\zeta^2/r_0$. Proceeding exactly as we did before in the far-zone approximation, we form the moment as the four-fold integral over the dummy space variables $\underline{x}^1 \ldots \underline{x}^4$ and interchange expectation and integration operations. Again we recognize that for large k, significant contributions to the moment are made only in the vicinity of the "stationary" points defined by (8). The moment M is thus decomposable as $M \simeq M_1 + M_2$ where M_1 and M_2 represent the contributions from S_1 and S_2. Again, we consider the integration over the volume surrounding the S_1 points. Transforming to the lag variables $\underline{u}$, $\underline{v}$, and $\underline{w}$ as per (9), and taking the limit, we get for the contribution from S_1

$$\lim_{k\to\infty} M_1 = M_1(\underline{K}; \Delta t) = (2r_0\cos^2\theta)^{-4} \iint G^2(\underline{x} + \underline{w})G^2(\underline{x} - \underline{V}\Delta t)$$

$$\cdot \, \Xi(K; \underline{w}) \exp[-i\underline{K}\cdot(\underline{w} + \underline{V}\Delta t)] \, \exp\big\{i(\kappa/r_0)$$

$$\cdot \, [\cos^2\theta(x_1 + w_1)^2 - (x_1 - V_1\Delta t)^2 + (x_2 + w_2)^2$$

$$- (x_2 - V_2\Delta t)^2]\big\} \, d\underline{x} \, d\underline{w} \qquad (72)$$

where we have taken the coordinates x_1 and x_2 of $\underline{x}$ to be radar-fixed coordinates (x_1 in the plane of incidence). Let G be the separable Gaussian pattern given by (43). The integrating over $\underline{x}$ we get

$$M_1(\underline{K}; \Delta t) = (2r_0\cos^2\theta)^{-4} \int B(K; \underline{w} + \underline{V}\Delta t)$$

$$\cdot \, \Xi(K; \underline{w}) \exp[-i\underline{K}\cdot(\underline{w} + \underline{V}\Delta t)] \, d\underline{w} \qquad (73)$$

where

$$B(K; \underline{w}) = (A_0/2) \exp\left(-\frac{1}{2} b_a^2 w_a^2\right) \qquad (74)$$

and

$$b_1^2 = b_\rho^2 = L_\rho^{-2} + (KL_\rho/2r_0\sin\theta)^2\cos^4\theta$$

$$b_2^2 = b_\phi^2 = L_\phi^{-2} + (KL_\phi/2r_0\sin\theta)^2$$

$$A_0 = \pi L_\rho L_\phi/2 \tag{74'}$$

and w.iere again the summation convention is applied to repeated indices.

Since $M = M_1 + M_2$, then N as given by (70) is similarly composed, i.e., $N = N_1 + N_2$ where N_1 and N_2 are the respective FT's of M_1 and M_2. From (70) we have

$$N_1(\underline{K};\Omega) = (2r_0\cos^2\theta)^{-4} \int d\underline{w}\, \Xi(K;\underline{w}) \exp(-i\underline{K}\cdot\underline{w})$$

$$\times \left\{ (2\pi)^{-1} \int d\Delta t\, B(K;\underline{w}+\underline{V}\Delta t)\exp[i(\Omega - \underline{K}\cdot\underline{V})\Delta t] \right\} \tag{75}$$

Let $\underline{W} = (b_1 w_1, b_2 w_2)$, $\underline{V} = (b_1 V_1, b_2 V_2)$ and $\Omega_* = \Omega - \underline{K}\cdot\underline{V}$. Then integrating over Δt we get

$$N_1(\underline{K};\Omega) = \frac{(A_0/2)}{(2r_0\cos^2\theta)^4} \int d\underline{w}\, \Xi(K;\underline{w})\exp(-i\underline{K}\cdot\underline{w})$$

$$\times \left\{ \frac{\exp\left[-\frac{1}{2}(\Omega_*/V)^2\right]}{\sqrt{2\pi}V} \cdot \exp\left[-\frac{1}{2}W^2\sin^2(\underline{V}, \underline{W})\right] \right.$$

$$\left. \cdot \exp[iW\cos(\underline{V}, \underline{W})\,\Omega_*/V] \right\} \tag{76}$$

From (70) and the inverse FT relationship, it follows that

$$M_1(\underline{K};0) = \int N_1(\underline{K};\Omega)\, d\Omega$$

$$= (2r_0\cos^2\theta)^{-4} \int B(K;\underline{w})\, \Xi(K;w)\, e^{-i\underline{K}\cdot\underline{w}}\, d\underline{w} \tag{77}$$

which is the same as the Fraunhofer solution (20), except that the Fresnel lag window $B(K;\underline{w})$ replaces the Fraunhofer lag window $A(w)$. Since B is not significantly sharper than A and the window can still be considered to be broad compared to the scale of variation in Ξ (i.e., broad compared to

the dominant wavelength $2\pi/K_o$), then $M_1(\underline{K}; 0)$ can be regarded as identical to the Fraunhofer moment $M_1(\underline{K})$. (Note that $B(0; \underline{w}) = A(\underline{w})$ and $B(K; \underline{Q}) = A(\underline{Q}) = A_o/2$.) If the detailed behavior of $N_1(\underline{K}; \Omega)$ near the origin $\underline{K} = 0$ is ignored, then it is apparent from (76) and (77) that N_1 is well approximated by

$$N_1(\underline{K}; \Omega) \simeq M_1(\underline{K}) \cdot \frac{\exp\left[-\frac{1}{2}(\Omega_a/\beta_{res})^2\right]}{\sqrt{2\pi}\,\beta_{res}}$$

where M_1 is given by (46) *et seq.*, and

$$\beta_{res} \stackrel{def.}{=} |\underline{V}| = (b_a V_a)^{\frac{1}{2}} = (b_\rho^2 \cos^2\Phi + b_\phi^2 \sin^2\Phi)^{\frac{1}{4}} \cdot V \qquad (79)$$

where Φ is the radar azimuth relative to the velocity vector $\underline{V}$. In A-H, only the line-broadening due to wave-front curvature was considered; i.e., it was assumed that $\beta_{res} \simeq \kappa LV/r_o$. However, to be accurate, the broadening due to the finite footprint must be accounted for also. Thus, compare V/L and $\kappa LV/r_o$ for typical aircraft and satellite geometries and ocean wavelengths: both terms are comparable.

The moment $M(k, \Delta k, \kappa; \Delta t)$ is not symmetric with respect to a κ and Δk interchange, and so the M_2 component (deriving from the S_2 stationary points) cannot simply be equated to M_1, as was possible in the time-independent case. Rather than labor through a solution for M_2 in these pages, we merely outline the key steps in the solution and indicate the appropriate assumptions and approximations: lag variables appropriate to the S_2 integration are defined, and the $k \to \infty$ limit is taken in the formation of Ξ; on account of the moderate bandwidth assumption (3″), the Fresnel phase terms in κ and Δk are neglected; assuming a large footprint area, we neglect the variation of Ξ near the origin and let $\Xi(0, \underline{w}) \simeq \Xi(0, \infty) = p_{V_\zeta}^2(\underline{s})$ in the integration over $\underline{w}$. Then, on taking the FT of M_2, we get

$$N_2 \simeq [\langle|S(k)|^2\rangle]^2 \exp\left[-\frac{1}{2}(q\Delta KL_\rho)^2\right] \cdot$$

$$\cdot \frac{\exp\left[-\frac{1}{2}(\Omega_a/\beta_d)^2\right]}{\sqrt{2\pi}\,\beta_d} \cdot \exp(i\epsilon\Omega_a/\beta_d^2) \qquad (80)$$

where

$$q = |\sin\Phi| \cdot [(L_\rho/L_\phi)^2\cos^2\Phi + \sin^2\Phi]^{-\frac{1}{2}}$$

$$\beta_d = (2kV/r_o) \cdot [L_\rho^2\cos^4\theta\cos^2\Phi + L_\phi^2\sin^2\Phi]^{\frac{1}{2}}$$

$$\epsilon = (2kV/r_o) \cdot \Delta K L_\rho^2\cos^2\theta\cos\Phi \tag{81}$$

and where $\Delta K \equiv 2\Delta k\sin\theta \equiv 2(\Delta\nu/c)\sin\theta$, and where again $\Omega_* = \Omega - \underline{K} \cdot \underline{V}$. As a check on (80) we have

$$\int_{-\infty}^{\infty} N_2 d\Omega = [\langle |S(k)|^2\rangle]^2 \exp\left[-\frac{1}{2}(\Delta K L_\rho)^2\right] \tag{82}$$

which is $M_1(\Delta\underline{K})$ with the weak modulation contribution neglected.

7. Results: Narrowband DF Technique

The spectrum of the narrowband DF signal, eq. (62), is simply N with ΔK set equal to zero in N_2. If a signal of finite record length T_{int} is passed to a spectrum analyzer or, equivalently, if a Bartlett lag window is applied to a measured covariance function $\hat{M}$ in a Tukey analysis (Blackmann and Tukey, 1958), then the measured spectrum will be (on the average)

$$\tilde{P}(\underline{K}) = \int W(\Omega - \underline{K} \cdot \underline{V})N(k, \underline{K}, \underline{0}; \Omega) d\Omega \tag{83}$$

where the spectral window is given by (66). If T_{int} is chosen such that $\beta_{res} T_{int} << 2\pi$, then from (78), (45), and (80) we have approximately

$$\tilde{P}(\underline{K}) \equiv \tilde{P}_1 + \tilde{P}_2 \simeq W(0)\int N_1 d\Omega + N_2(0)\int W d\Omega$$

$$\simeq (1) \cdot \frac{\sqrt{2\pi}}{L_\rho} P_{mod}(\underline{K}) + \left(\frac{1}{\sqrt{2\pi}\beta_d}\right)\left(\frac{2\pi^2}{T_{int}}\right) \tag{84}$$

For example, let us set $T_{int} = \beta_{res}^{-1}$. Then the measurement signal-to-noise ratio is

$$SNR \equiv \tilde{P}_1/\tilde{P}_2 = (2\pi)^{-3/2}\left(\frac{\beta_d}{\beta_{res}}\right) \cdot \frac{\sqrt{2\pi}}{L_\rho} P_{mod}(\underline{K}) \tag{85}$$

where we have let P_{mod} become the one-sided spectrum; i.e., we have let $P_{mod} \leftarrow 2P_{mod}$. With the same parameter values used previously in the modulation noncoherent analysis, i.e., $\theta = 12.5°$,

$L_\rho = 5.0$ km, $L_\phi = 2.5$ km, $|\underline{K}| = 2\pi/200$ m, $U = 18$ ms^{-1}, we have as before $(\sqrt{2\pi}/L_\rho)P_{mod}(\underline{K}) = -36$ dB. Now, if $k = 2\pi/2$ cm, $r_0 = 700$ km and $V = 7$ kms^{-1}, then e.g. for broadside looks, $\Phi = \pm 90°$, we have

$$\beta_{res} = [(V/L_\phi)^2 + (KL_\phi V/2r_0 \sin\theta)^2]^{\frac{1}{4}}$$

$$= [7.84 \text{ s}^{-2} + 3.29 \text{ s}^{-2}]^{\frac{1}{4}} = 3.34 \text{ s}^{-1}$$

$$\beta_d = 2kL_\phi V/r_0 = 1.57 \times 10^4 \text{ s} \tag{86}$$

The filtering gain is $(2\pi)^{-3/2}(\beta_d/\beta_{res}) = 25$ dB. Hence, the final measurement SNR is

$$SNR_{DF} = -36 \text{ dB} + 25 \text{ dB} = -11 \text{ dB} \tag{87}$$

Of course, this SNR figure can be improved upon by designing a spectral analysis having a better "match" to the resonance peak (e.g., by using a matched filter). However, it is apparent that, at best, given reasonable parameter values, the SNR will not much exceed 0 dB.

8. Results: SP Technique

Making use of the transformations (55) *et seq.*, we express our results (78) and (80) in terms of frequency. For $|\omega| > 0$ (i.e., ignoring the dc), we have $N(\nu, \Delta\nu, \omega; \Omega) = N_1 + N_2$,

$$N_1 = [\langle|S(\nu)|^2\rangle]^2 \exp\left[-\frac{1}{2}\left(\frac{\Omega_*}{\beta_{res}}\right)^2\right] \cdot \frac{\sqrt{2\pi}}{T_r} P_{mod}(\omega, \Phi) \tag{88a}$$

$$N_2 = [\langle|S(\nu)|^2\rangle]^2 \exp\left[-\frac{1}{2}\left(\frac{\Omega_*}{\beta_d}\right)^2\right] \exp\left[-\frac{1}{2}(q\Delta\nu T_r)^2\right] \exp(i\epsilon\Omega_*/\beta_d) \tag{88b}$$

If the pulse bandwidth is large compared to $(qT_r)^{-1}$, then N_2 behaves as a delta function in $\Delta\nu = \nu-\nu'$. Hence, since $\langle|S(\nu)|^2\rangle$ is practically a constant over the pulse bandwidth, eq. (71) becomes

$$P(\omega, \Omega) \equiv P_1 + P_2$$

$$= N_1 \cdot |\int E_0(\nu)E_0^*(\nu-\omega)d\nu|^2$$

$$+ [\int E_0^2(\nu)E_0^2(\nu-\omega)d\nu] \cdot \int N_2 d\Delta\nu \tag{89}$$

Making use of the definitions (81) and the identity $\Delta KL_\rho = \Delta\nu T_r$ we have for the N_2 integration,

$$\int N_2 d\Delta\nu = (\sqrt{2\pi}/T_r)[\langle|S(\nu)|^2\rangle]^2 \cdot \frac{\exp\left[-\frac{1}{2}(\Omega_*/q\beta_d)^2\right]}{\sqrt{2\pi}\,q\beta_d} \tag{90}$$

where (from 81),

$$q\beta_d = (2kV/r_0)\,L_\phi\,|\sin\Phi| \tag{91}$$

which is the Doppler spread due to azimuthal aspect variation alone.

Pulse waveforms are often Gaussian in shape; let $E_0(\nu)$ at baseband be given by

$$E_0(\nu) = \frac{\exp\left[-\frac{1}{2}(\nu/\beta_p)^2\right]}{\sqrt{2\pi}\,\beta_p} \tag{92}$$

Then, computing the integrals in (87), we have

$$P(\omega,\Omega) = P_1 + P_2 = \frac{\sqrt{2\pi}}{T_r}[\langle|S(\nu)|^2\rangle]^2 \cdot \frac{\exp\left[-\frac{1}{2}(\omega/\beta_p)^2\right]}{4\pi\beta_p^2} \cdot$$

$$\times \left\{ \frac{\exp\left[-\frac{1}{2}(\Omega_*/\beta_{res})^2\right]}{\sqrt{2\pi}\,\beta_{res}} \cdot P_{mod}(\omega,\Phi) + \frac{\exp\left[-\frac{1}{2}(\Omega_*/q\beta_d)^2\right]}{2\pi\,q\beta_p\beta_d} \right\} \tag{93}$$

The post-detection "pulse-Doppler" spectrum $P(\omega,\Omega)$ is sketched in Figure 7.

Except for looks directly forward ($\Phi = 0°$) or aft ($\Phi = 180°$), $q\beta_d \gg \beta_{res}$. Hence, in the vicinity of the resonance peak at $\Omega = \underline{K} \cdot \underline{V}$ we can set $\Omega_* = 0$ in P_2. Again, if we assume short integration times, T_{int}, such that the resonance peak is entirely covered by the spectral window W, i.e. if $\beta_{res}T_{int} \ll 2\pi$, the filtered pulse spectrum becomes (cf. 65),

$$\tilde{P}(\omega) = \tilde{P}_1 + \tilde{P}_2 \simeq W(0)\int P_1 d\Omega + P_2 \int W d\Omega \tag{94}$$

Again, assuming $T_{int} = \beta_{res}^{-1}$, from (93) we have

$$SNR_{SP} = \tilde{P}_1/\tilde{P}_2 = (2\pi)^{-3/2}\left(\frac{q\beta_d}{\beta_{res}}\right) \cdot \sqrt{2\pi}\,\beta_p\,P_{mod}(\omega,\Phi) \tag{95}$$

Again, we assume the same familiar parameter values (cf. Table I). Then, as before, we have

$$\sqrt{2\pi}\,\beta_\rho\, P_{mod}(\omega, \Phi) \equiv (\sqrt{2\pi}/\Delta_\rho)\, P_{mod}(\underline{K}) = -6\ dB \qquad (96)$$

For broadside looks ($\Phi = \pm 90°$), we have $\beta_{res} = 3.34\ s^{-1}$ (from 86a) and $q\beta_d = 1.57 \times 10^4\ s^{-1}$ (from 86 and 91). Hence,

$$SNR_{SP} = 25\ dB - 6\ dB = +19\ dB \qquad (97a)$$
$$\text{(broadside)}$$

For looks $\pm 1°$ of forward or aft, $\beta_{res} = 2.23\ s^{-1}$ and $q\beta_d = 2.74 \times 10^2\ s^{-1}$; in this case,

$$SNR_{SP} = 9\ dB - 6\ dB = +3\ dB \qquad (97b)$$
$$\text{(fore/aft)}$$

9. Discussion

In the foregoing analysis, the backscattered signals were assumed to be continuous functions of slow time t. Such an assumption will be valid only if the pulse repetition frequency (PRF) is greater than or equal to the rate of the fastest signal fluctuation determined by the Doppler spread (i.e., determined by β_d in the narrowband DF measurement (beam-limited illumination), or determined by $q\beta_d$ in the SP measurement (pulse-limited illumination)). If the PRF is lower than the Doppler fading rate, then signal fluctuation power at frequencies greater than one-half the PRF (the Nyquist frequency) must appear in the frequency band 0 – ½ PRF. The pulse Doppler spectrum $P(\omega, \Omega)$ at multiples of the Nyquist frequency, will be folded over onto the interval 0 – ½ PRF (Blackman and Tukey, 1958). This folding over will result in an increased measured signal fading spectrum, the increase being roughly in proportion to the ratio of the Doppler spread to the PRF. Clearly, in the case of the narrowband DF measurement, where the SNR is already poor in the continuously sampled case, one cannot very well afford to undersample. In the SP measurement, on the other hand, one starts with a generous SNR in the continuously sampled case, and one can easily afford to lower the PRF. Clearly, the designer of an SP instrument will be able to select and trade off pulse bandwidth, integration time, and PRF parameters with a fair degree of freedom; he will also have some flexibility in terms of antenna gain and azimuth scan rate parameters.

We have not undertaken to describe or analyze a possible modulation coherent wide' and DF system. Our experience with the modulation noncoherent wideband DF system, however, would indicate that such a system would perform comparably to an SP system.

We have not considered thermal noise in our analysis, mainly for the reason that thermal noise will not be a limiting factor unless it equals or exceeds the average backscattered power level. Available transmitters (e.g., the one in the Seasat-1 altimeter (Townsend, 1980)) have enough power to deliver a unity-or-better signal-to-thermal noise ratio when modest gain antennas are used and the nadir angle is about $10°$.

We have not given any figures for directional resolution; some actual numbers may be enlightening. These numbers can be derived from the Fresnel lag window $B(K; \underline{w})$, eq. (74). If we consider only the linear term in $\Xi(K; \underline{w})$ (in which the exponential factor is neglected), and if we assume $K \gg b_a$, $a = 1, 2$, then it is apparent that the spectral window through which the slope spectrum $K^2 F(\underline{K})$ is seen is given approximately by the FT of $B(K; \underline{w})$ with respect to $\underline{w}$. The one-sigma values of the Gaussian-shaped window in range ($a = 1$) and azimuth ($a = 2$) are respectively given by b_a. Using the familiar parameter values of Table 1, and defining directional resolution as the half-power window width in azimuth, we have

$$\Delta\Phi = 2\sqrt{2\ln 2}\, b_\phi / K$$
$$= 2\sqrt{2\ln 2}\, [(KL_\phi)^{-2} + (L_\phi/2r_0\sin\theta)^2]^{\frac{1}{2}}$$
$$= (2.36) \cdot [1.6 \times 10^{-4} + 1.3 \times 10^{-5}]^{\frac{1}{2}}$$
$$= 0.031 \text{ rad} = 1.8 \text{ deg.} \tag{98}$$

For the main reason that the diffraction fields in near-vertical backscatter are both small and diffuse compared to the GO (geometrical optics) fields, I believe that the GO solution for the modulation spectrum given here (or the same, the non-dc portion of the spectrum of the impulse response) is an accurate one, at least for incidence angles less than $15°$. The expansion of $\Xi(K; \underline{w})$ to the first order in non-Gaussian statistics (i.e., third order moments) and to the second order in Gaussian statistics is, I believe, a reasonable and consistent approach to take. By expanding Ξ (asymptotically,

for large lags) one has immediately a linear term that is directly proportional to the directional wave slope spectrum, with a proportionality factor that agrees with the simplest tilting model of reflectivity modulation (cf. Fig. 2). Also, by using an expansion technique, one has a method, in principle at least, for solving the inverse problem: the raw observations can be used to give a first estimate of the true directional height or slope spectrum which, in turn, can be used in a forward prediction of the higher-order terms. Since those terms are small, one iteration would probably suffice. Still, a means of handling the non-Gaussian terms in a theoretical sense and in a practical sense (i.e., in terms of developing a viable algorithm) needs to be invented.

While the expansion of $\Xi(K; \underline{w})$ is certainly valid for large lags $\underline{w}$, it does not follow that the expansion of $M_1(\underline{K})$ is similarly valid, as stated in the abstract of this paper. Since Ξ is not accurately represented for small lags, then $M_1(\underline{K})$, as the FT of Ξ with respect to $\underline{w}$, will be uncertain in terms of the absolute degree of whitening caused by the fine structure of Ξ near the origin. Until this representation problem has been solved, or at least until quantitative error bounds have been established, the sample calculations given in Fig. 5 must be regarded as semi-quantitative.

10. Conclusion

We have shown, theoretically, how rather simple, scanning-beam, microwave radars can be used to measure directional ocean wave spectra from satellite platforms. The theory indicates that: (1) The short-pulse (SP) approach to the measurement is superior to the narrowband dual-frequency (DF) approach in terms of measurement signal-to-noise ratio (SNR) and contrast ratio (CR), and in terms of the added flexibility in overall design that the greater SNR and CR figures of the SP approach afford. (2) Conceivibly, wideband DF systems may be designed that perform comparably to wideband SP systems. (3) The radar-observed surface spectrum bears rather good fidelity to the directional slope spectrum in the incidence angle range $8° \leq \theta \leq 15°$ provided that the wind speed is not to low ($U \gtrsim 5$ ms^{-1}) and provided that the large wave steepness is not too great ($\delta_0 \lesssim 0.1$). In principle, based on the theoretical model presented here, algorithms can be written to remove the small amount of harmonic distortion inherent in the specular scatter measurement of the sea slope

spectrum. Such algorithms, it is believed, will have to take account of the effects of non-Gaussian water wave statistics, as it appears that the effects of non-Gaussian wave statistics are comparable to those existing in the second order of scattering from a normally distributed sea. A better understanding of the measurement problem — to this level of detail — will clearly require much additional analysis work and experimentation.

In a companion paper (Jackson *et al.*, 1980, in this issue), experimental aircraft data are presented that support the basic findings of the present theoretical investigation: namely, that directional wave slope spectra can be measured with rather good fidelity from near-vertical measurements of microwave backscatter, remotely, using a scanning beam, short-pulse radar system.

ACKNOWLEDGMENT

APPENDIX A: Analysis of SP and DF Systems

Consider the SP system of Fig. 3a. If the FT of the backscattered field is given by $E_s(\nu) = S(\nu) E_0(\nu)$, then the FT of the square-law detected signal is

$$P(\omega) = \int_{-\infty}^{\infty} S(\nu) S^*(\nu - \omega) E_0(\nu) E_0^*(\nu - \omega) \, d\nu \qquad (A1)$$

The ensemble average output of the spectrum analyzer is the pulse spectrum $P(\omega) = \langle |P(\omega)|^2 \rangle$ as seen through the H_i bandpass filter; i.e., $P_{out}(\omega_i) = (2\pi)^3 \int |H_i(\omega)|^2 P(\omega) d\omega$. If the analysis bandwidth β_{ai} of the H_i filter is small compared to the variation in $P(\omega)$, then $P_{out}(\omega_i) \propto \beta_{ai} P(\omega_i)$. From (A1) we have

$$P(\omega) = \iint_{-\infty}^{\infty} M(\nu, \nu', \omega) \, E_0(\nu) \, E_0^*(\nu - \omega) \, E_0^*(\nu') \, E_0(\nu' - \omega) \, d\nu d\nu' \qquad (A2)$$

where

$$M = \langle S(\nu) S^*(\nu - \omega) S^*(\nu') S(\nu' - \omega) \rangle \qquad (A3)$$

The moment M is given by (55) and (56)

$$M = (\sqrt{2\pi}/T_r) \, [\langle |S(\nu)|^2 \rangle]^2 \cdot \{ \delta(\omega) + \delta(\Delta\nu) + P_{mod}(\omega) + P_{mod}(\Delta\nu) \} \qquad (A4)$$

where $\Delta\nu = \nu - \nu'$. For weak modulation, $\int P_{mod}(\Delta\nu) d\Delta\nu \ll 1$, and we can neglect the contribution of $P_{mod}(\Delta\nu)$ to $P(\omega)$; since $\langle |S(\nu)|^2 \rangle$ is practically a constant over the few percent pulse bandwidths we are considering, we then have on substituting (A4) into (A2):

$$P(\omega) \simeq (\sqrt{2\pi}/T_r) \, [\langle |S(\nu)|^2 \rangle]^2 \, \{ |\int E_0(\nu) E_0^*(\nu - \omega) d\nu|^2 \cdot$$

$$\cdot \, [\delta(\omega) + P_{mod}(\omega)] + \int E_0^2(\nu) E_0^2(\nu - \omega) d\nu \} \qquad (A5)$$

Pulse waveforms are often Gaussian in shape; let the FT of the envelope of the incident waveform be given by

$$E_0(\nu) = \exp\left[-\frac{1}{2} (\nu/\beta_p)^2 \right] \Big/ \sqrt{2\pi} \, \beta_p \qquad (A6)$$

Then $P(\omega)$ has the form

$$P(\omega) \simeq (\sqrt{2\pi}/T_r)\, [\langle |S(\nu)|^2 \rangle]^2 \cdot \frac{\exp\left[-\frac{1}{2}\,(\omega/\beta_p)^2\right]}{4\pi\,\beta_p^2} \cdot$$

$$\cdot \left| \delta(\omega) + \frac{1}{\sqrt{2\pi}\,\beta_p} + P_{mod}\,(\omega, \Phi) \right| \tag{A.7}$$

Now, consider the DF system diagrammed in Fig. 3b. The H_i and H_j are non-overlapping bandpass filters with center frequencies ν_i and ν_j, respectively; the K_i and K_j are dc blocking filters. The output of the correlator can be written as

$$P_{out}(\nu_i - \nu_j) = (2\pi)^3 \int K_i(\omega)\, K_j^*(\omega)\, \langle P_i P_j^* \rangle \, d\omega$$

$$\langle P_i P_j^* \rangle = (2\pi)^4 \iint M(\nu, \nu', \omega)\, H_i(\nu)\, E_o(\nu) \cdot$$

$$\cdot H_i^*(\nu - \omega)\, E_o^*(\nu - \omega)\, H_j^*(\nu')\, E_o^*(\nu')\, H_j(\nu' - \omega)\, E_o(\nu' - \omega)\, d\nu\, d\nu' \tag{A8}$$

where M is given by (A4). Since the K filters block dc, $K_i(0) = K_j(0) = 0$; let $K_i = K_j = (2\pi)^{-1}$, for $\omega > 0$. Then, assuming that the H-filters are non-overlapping and that the bandwidths β_{ai} and β_{aj} are narrow compared to the variation in P_{mod}, we have using (A4), approximately,

$$P_{out} \simeq (2\pi)^5\, P_{mod}(\nu_i - \nu_j) \cdot \int H_i H_j^*\, d\omega \tag{A9}$$

where $H_i(\omega) = \int H_i(\nu)\, E_o(\nu)\, H_i^*(\nu - \omega)\, E_o^*(\nu - \omega)\, d\nu$ ($i \to j$). Two waveforms of interest are SP waveforms and DF waveforms that are matched to the H-filters. For SP waveforms, E_o is constant over the bandpasses of the H_i filters. If the filter functions are Gaussian with standard deviations β_{ai} and β_{aj}, then

$$P_{out} \propto \beta_{aij}\, P(\Delta\nu_{ij}) \tag{A10}$$

where $\Delta\nu_{ij} = \nu_i - \nu_j$ and $\beta_{aij} = \beta_{ai}\beta_{aj}(2\beta_{ai}^2 + 2\beta_{aj}^2)^{-\frac{1}{2}}$. A similar analysis may be carried out for the case where the receiver filters are matched to the transmitter waveform; e.g., if the DF waveform is $E_o = E_{oi} + E_{oj}$ then $H_i = E_{oi}^*$ ($i \to j$).

APPENDIX B: Alternative Derivation of PO Limit

The fact that Eq. (7) has the unique stationary points given by (8), of course, has to do with the smoothness and extremal properties of the mathematical expectation, i.e., the factor in braces. The following development may clarify this point. Consider the second moment of S(k) in the case of backscatter in two dimensions only. Then, we must evaluate the following integral in the limit $k \rightarrow \infty$:

$$I_k = 2k\cos\theta \int_{-\infty}^{\infty} \langle e^{-i2k\cos\theta \, [\zeta(w)-\zeta(0)]} \rangle \, e^{-i2k\sin\theta \, w} \, dw \qquad (B1)$$

Let $z = [\zeta(w) - \zeta(0)]/w$ and let $p_z(z; w)$ be the pdf of z. Then

$$I_k = 2k\cos\theta \iint_{-\infty}^{\infty} p_z(z; w) \, e^{i2k\cos\theta \, (z-\tan\theta)w} \, dz\,dw \qquad (B2)$$

Since p_z is a slowly varying function of z and w, we can apply the method of stationary phase. A saddle point exists at $z = \tan\theta$ and $w = 0$. Letting

$$u = (z - \tan\theta + 2k\cos\theta w)/\sqrt{2}$$

$$v = (z - \tan\theta - 2k\cos\theta w)/\sqrt{2}$$

then since $\lim_{w \to 0} z = \zeta_x$ where ζ_x is the surface slope and since $\lim_{w \to 0} p_z = p_{\zeta_x}$ it follows that

$$\lim_{k \to \infty} I_k = p_{\zeta_x}(\tan\theta) \cdot \iint_{-\infty}^{\infty} e^{i[(u^2-v^2)/2]} \, du\,dv$$

$$= 2\pi \, p_{\zeta_x}(\tan\theta) \qquad (B3)$$

which result agrees with Barrick (1968b).

APPENDIX C: Second-order Terms in the Expansion of $M_1(\underline{K})$

The second-order terms in the expansion of $\psi_{\underline{\xi}}$, eq. (38), are:

$$\frac{1}{2}\left[\frac{1}{2}\,^o\mu^{(2)}_{ij}\,t_i t_j\right]^2 = \frac{1}{8}\,^o\mu^{(2)}_{ij}\,^o\mu^{(2)}_{k\ell}\,t_i t_j t_k t_\ell$$

$$= \frac{1}{2}\left[(K\cot\theta)^4\,R^2 + R_{,\alpha\beta}\,R_{,\gamma\delta}\,u_\alpha u_\delta\,v_\beta v_\gamma + \right.$$

$$+ (K\cot\theta)^2\,R_{,\alpha}\,R_{,\beta}\,(u_\alpha u_\beta - 2u_\alpha v_\beta + v_\alpha v_\beta) -$$

$$- 2(K\cot\theta)^2\,R\,R_{,\alpha\beta}u_\alpha v_\beta + 2(K\cot\theta)^3\,R\,R_{,\alpha}\,(u_\alpha - v_\alpha) -$$

$$\left. - 2(K\cot\theta)\,R_{,\alpha\beta}\,R_{,\gamma}\,u_\alpha v_\beta\,(u_\gamma - v_\gamma)\right] \tag{C1}$$

Fourier transforming with respect to $\underline{u}$ and $\underline{v}$ according to eq. (21) and making use of the identities (39), we get for the second-order terms in the expansion of Ξ, eq. (40):

$$\frac{1}{2}(K\cot\theta)^4\,R^2 + \frac{1}{2}\frac{P_{,\alpha\delta}\,P_{,\beta\gamma}}{p^2}\,R_{,\alpha\beta}\,R_{,\gamma\delta}$$

$$-(K\cot\theta)^2\left(\frac{P_{,\alpha\beta}}{p} + \frac{P_{,\alpha}\,P_{,\beta}}{p^2}\right)\,R_{,\alpha}\,R_{,\beta} - (K\cot\theta)^2\,\frac{P_{,\alpha}\,P_{,\beta}}{p^2}\,R\,R_{,\alpha\beta}$$

$$+ 2i(K\cot\theta)^3\,\frac{P_{,\alpha}}{p}\,R\,R_{,\alpha} - iK\cot\theta\left(\frac{P_{,\alpha\gamma}\,P_{,\beta} + P_{,\beta\gamma}\,P_{,\alpha}}{p^2}\right)\,R_{,\alpha\beta}\,R_{,\gamma} \tag{C2}$$

From the definition of the height spectrum as the Fourier transform of the covariance function, viz.,

$$F(\underline{K}) \equiv FT\{R\} \equiv \frac{1}{(2\pi)^2}\int R(\underline{w})\,e^{-i\underline{K}\cdot\underline{w}}\,d\underline{w} \tag{C3}$$

it follows that the FT of the second-order terms in Ξ is given by various convolutions involving the height spectrum; e.g.,

$$FT\{R\,R_{,a}\} = FT\{R\} * FT\{R_{,a}\}$$

$$= F(\underline{K}) * \{iK_a\,F(\underline{K})\}$$

$$\equiv \int_{-\infty}^{\infty} F(\underline{K}')\,\{i(K'_a - K_a)\,F(\underline{K}' - \underline{K})\}\,d\underline{K}' \tag{C4}$$

If an overbar is used to distinguish a variable wavenumber entering into a convolution, then the second-order terms in the expansion of P_{mod}, eq. (48), are written as

$$+\frac{1}{2}\,(K\cot\theta)^4\,F * F + \frac{1}{2}\,\frac{P_{,a\delta}\,P_{,\beta\gamma}}{p^2}\,\overline{K_a\,K_\beta\,F} * \overline{K_\gamma\,K_\delta\,F}$$

$$+(K\cot\theta)^2\left(\frac{P_{,a\beta}}{p} + \frac{P_{,a}\,P_{,\beta}}{p^2}\right)\overline{K_a\,F} * \overline{K_\beta\,F} +$$

$$+(K\cot\theta)^2\,\frac{P_{,a}\,P_{,\beta}}{p^2}\,F * \overline{K_a\,K_\beta\,F} - 2(K\cot\theta)^3\,\frac{P_{,a}}{p}\,F * \overline{K_a\,F}$$

$$-K\cot\theta\left(\frac{P_{,a\gamma}\,P_{,\beta} + P_{,\beta\gamma}\,P_{,a}}{p^2}\right)\overline{K_a\,K_\beta\,F} * \overline{K_\gamma\,F} \tag{C5}$$

REFERENCES

Alpers, W. and K. Hasselmann (1978), The two-frequency microwave technique for measuring ocean wave spectra from an airplane or satellite, Boundary Layer Met., 13, 215-230.

Barrick, D. E. (1968a), Rough surface scattering based on the specular point theory, IEEE Trans. Antennas Propagat., AP-16, 449-454.

Barrick, D. E. (1968b), Relationship between slope probability density function and the physical optics integral in rough surface scattering, Proc. IEEE, October.

Barrick, D. E. (1974), Wind dependence of quasi-specular microwave sea scatter, IEEE Trans. Antenna Propagat., AP-22, 135-136.

Beckmann, P. and A. Spizzichino (1963), The Scattering of Electromagnetic Waves from Rough Surfaces, Pergamon Press, New York.

Blackman, R. B. and J. W. Tukey (1958), The Measurement of Power Spectra, Dover Publications, New York.

Brown, G. S. (1978), Backscattering from a Gaussian-distributed perfectly conducting rough surface IEEE Trans. Antenna Propagat., AP-26, 472-482.

Cox, C. and W. Munk (1954), Measurement of the roughness of the sea surface from photographs of the sun's glitter, J. Opt. Soc. Am., 44, 838-850.

Hasselmann, K., W. Munk and G. MacDonald (1963), Bispectra of ocean waves, Time Series Analysis (M. Rosenblatt, Ed.), John Wiley & Sons, New York.

Hasselmann, K. (1972), Radar backscatter from the sea surface, 8th Symp. Naval Hydrodyn., ARC-179, Office of Naval Research, Dept. of the Navy.

Huang, N. E. and S. R. Long (1980), An experimental study of the surface elevation probability distribution and statistics of wind generated waves, J. Fluid Mech., 101, 179-200.

Jackson, F. C. (1974a), A curvature-corrected Kirchoff formulation for radar sea-return from the near vertical, NASA CR-2406 to Langley Research Cntr., April.

Jackson, F. C. (1974b), Directional spectra of ocean waves from microwave backscatter, Proc. URSI Specialists Meeting Microwave Scattering and Emission from the Earth, (E. Shanda, Ed.), Berne, Switzerland, 23-26, September.

Jackson, F. C. (1979), The reflection of impulses from a nonlinear random sea, J. Geophys. Res., 84, (C8), 4939-4943.

Jones, W. L., L. C. Schroeder and J. L. Mitchell (1977), Aircraft measurements of the microwave scattering signature of the ocean, IEEE J. Oceanic Eng., OE-2, 52-61.

Longuet-Higgins, M. S. (1959), The distribution of the sizes of images reflected in a random surface, Proc. Camb. Phil. Soc., 55, 91-100.

Longuet-Higgins, M. S. (1963), The effect of nonlinearities on statistical distributions in the theory of sea waves, J. Fluid Mech., 17, 459-480.

Lynch, R. J. and R. J. Wagner (1970), Rough surface scattering: shadowing, multiple scatter, and energy conservation, J. Math. Phys., 11, 3032-3042.

Papoulis, A. (1965), Probability, Random Variables, and Stochastic Processes, McGraw-Hill Book Company.

Parzen, E. and N. Shiren (1956), Analysis of a general system for the detection of amplitude modulated moise, J. Math. Phys., 35, 278-288.

Plant, W. J. (1977), Studies of backscattered sea return with a CW dual frequency, X-band radar, IEEE Trans. Antennas Propagat., AP-25, 28-39.

Plant, W. J. and D. L. Schuler (1980), Remote sensing of the sea surface using one- and two-frequency microwave techniques, Radio Science, 15, (3), 605-615.

Ruck, G., D. E. Barrick and T. T. Kaliszewski (1972), Bistatic sea state monitoring, Battelle Columbus Labs Technical Report, Columbus, Ohio, June.

Schuler, D. L. (1978), Remote sensing of directional gravity wave spectra using a microwave dual frequency radar, Radio Science, 13, 321-331.

Tomiyasu, K. (1971), Short pulse wide-band scatterometer ocean surface signature, IEEE Trans. Geoscience Elec., GE-9, 175-177.

Townsend, W. F. (1980), An initial assessment of the performance achieved by the Seasat-1 radar altimeter, IEEE J. Oceanic Eng., OE-5, 80-92.

Valenzuela, G. R. (1978), Theories for the interaction of electromagnetic and oceanic waves – a review, Boundary Layer Met., 13, 61-85.

Valenzuela, G. R. and J. W. Wright (1979), Modulation of short gravity-capillary waves by longer-scale periodic flows – a higher order theory, Radio Science, 14, (6), 1099-1110.

Weissman, D. E. (1973), Two frequency radar interferometry applied to the measurement of ocean wave height, IEEE Trans. Antennas Propagat., AP-21, 649-656.

Wentz, F. J. (1978), Estimation of the sea surface's two-scale backscatter parameters, NASA CR-145255 to Langley Research Center, March.

Wilheit, T. T. (1979), The effect of wind on the microwave emission from the ocean's surface at 37 GHz, J. Geophys. Res., 84, (C8), 4921-4930.

Wright, J. W., W. J. Plant, W. C. Keller and W. L. Jones (1980), Ocean wave-radar modulation transfer functions from the West Coast Experiment, J. Geophys. Res., 85, (C9), 4957-4966.

FIGURE CAPTIONS

Fig. 1.   Overall geometry and coordinate definition.

Fig. 2.   Simple tilt model of reflectivity modulation.

Fig. 3.   (a) Schematic of modulation noncoherent short pulse system. (b) Diagram of wideband

dual frequency system (after Parzen and Shiren, 1956)

Fig. 4.   Possible realization of a modulation coherent short pulse system. τ denotes fast signal

time and t slow signal time. The slow time filter can be realized by a sample-and-hold

that is triggered at successive delays given by $\dot{\tau}$t, followed by an accumulator. The spec-

trum analyzer can be realized by digitally fast Fourier transforming the slow time

filtered pulse return, and squaring the magnitude.

Fig. 5.   Sample calculations of the spectrum $P_{mod}(K)$ of backscattered impulses from a Gaussian

sea surface in two dimensions in the second order of scattering. (a, b) The surface slope

spectrum $K^2 F(K)$ is the Phillips spectral form, BK^{-1}, with an abrupt cutoff at $K = K_o$.

The slope spectrum and P_{mod} are both normalized by their values at K_o. The calculations

are performed for a range of wave steepness $\delta_o = K_o \sigma = \sqrt{B/2}$, incidence angle θ and wind

speed U (which determines the total mean square slope according to eq. (30)). In all cal-

culations, the location of the peak at K_o is preserved; low frequency whitening – or inter-

modulation (IM) – is exhibited; and the frequency response (FR) at wavenumbers $K > K_o$

is in the form of a droop. Panels (c-e) show the variation of the IM at $K = 0.5 K_o$ and the

FR at $K = 2 K_o$ over the range of parameter values indicated.

Fig. 6.   Spectrum of backscattered power when a short pulse of bandwidth β_p is transmitted, and

definition of the SNR.

Fig. 7.   Post-detection "pulse-Doppler" spectrum.

Table I. Parameter Values Used in Sample Calculations

Incidence angle	$\theta = 12.5°$
Slant range	$r_o = 700$ km
Satellite velocity	$V = 7$ kms^{-1}
Beam spot size* in range	$L_\rho = 5.0$ km
Beam spot size* in azimuth	$L_\phi = 2.5$ km
EM wavenumber	$k = 2\pi/2$cm
Water wavenumber	$K = 2\pi/200$ m
Wind speed	$U = 18$ ms^{-1}
Pulse bandwidth parameter[†]	$\beta_p = 1.4 \times 10^8$ s^{-1}
Surface range resolution parameter	$\Delta\rho = 5$ m

*One-sigma value of Gaussian, one-way power pattern

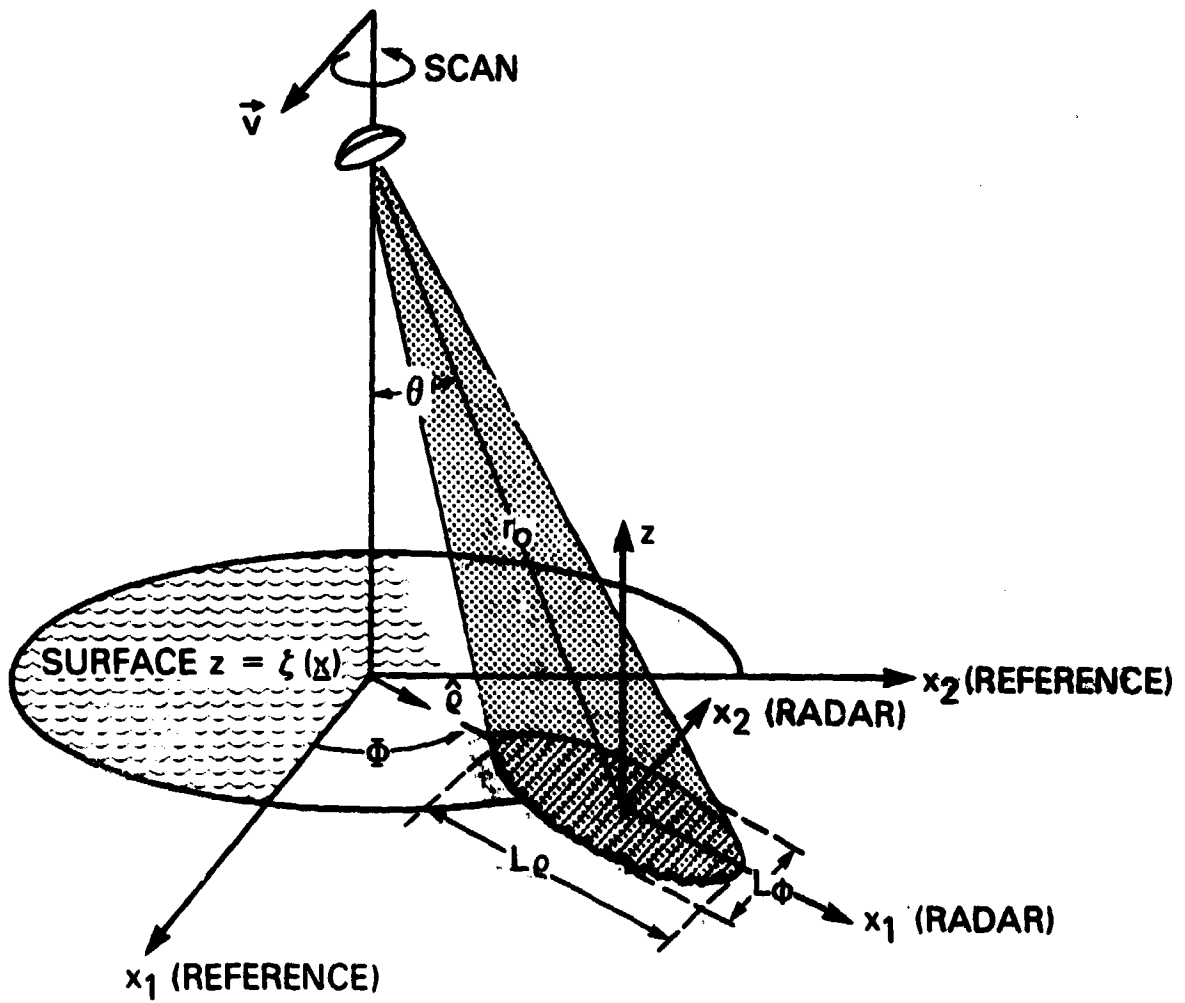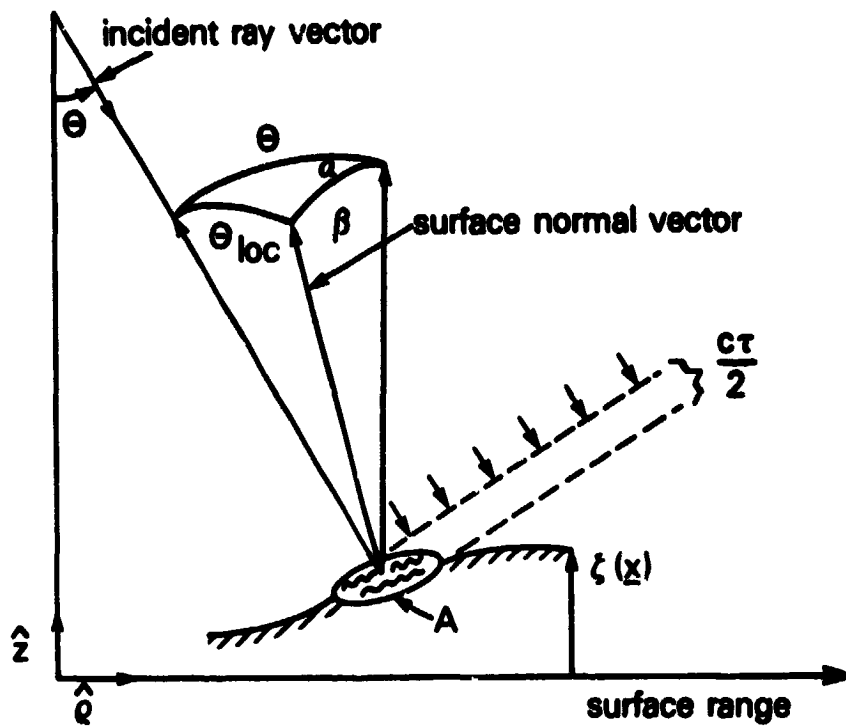[†]One-sigma value of Gaussian envelope of field strength

Figure 1

The fractional backscatter cross-section variation is

$$\frac{\delta\sigma}{\sigma} = \frac{\delta(\sigma^o A)}{\sigma^o A} = \frac{\delta\sigma^o}{\sigma^o} + \frac{\delta A}{A}$$

Assume that $\sigma^o = \pi \sec^4\Theta\, p(s)$ where $s = \tan\Theta_{loc}$ and p is the slope pdf. From the spherical triangle, if $\Theta \gg \beta$, it follows that $\Theta_{loc} \sim \Theta - \beta\cos\alpha$; or $\Theta_{loc} \sim \Theta - \hat{\rho}\cdot\nabla\zeta$. Since $A \propto c\tau/2\sin\Theta_{loc}$ it follows that

$$\frac{\delta\sigma}{\sigma} = \left(\cot\Theta - \frac{\partial \ell n p}{\partial s}\right)\hat{\rho}\cdot\nabla\zeta$$
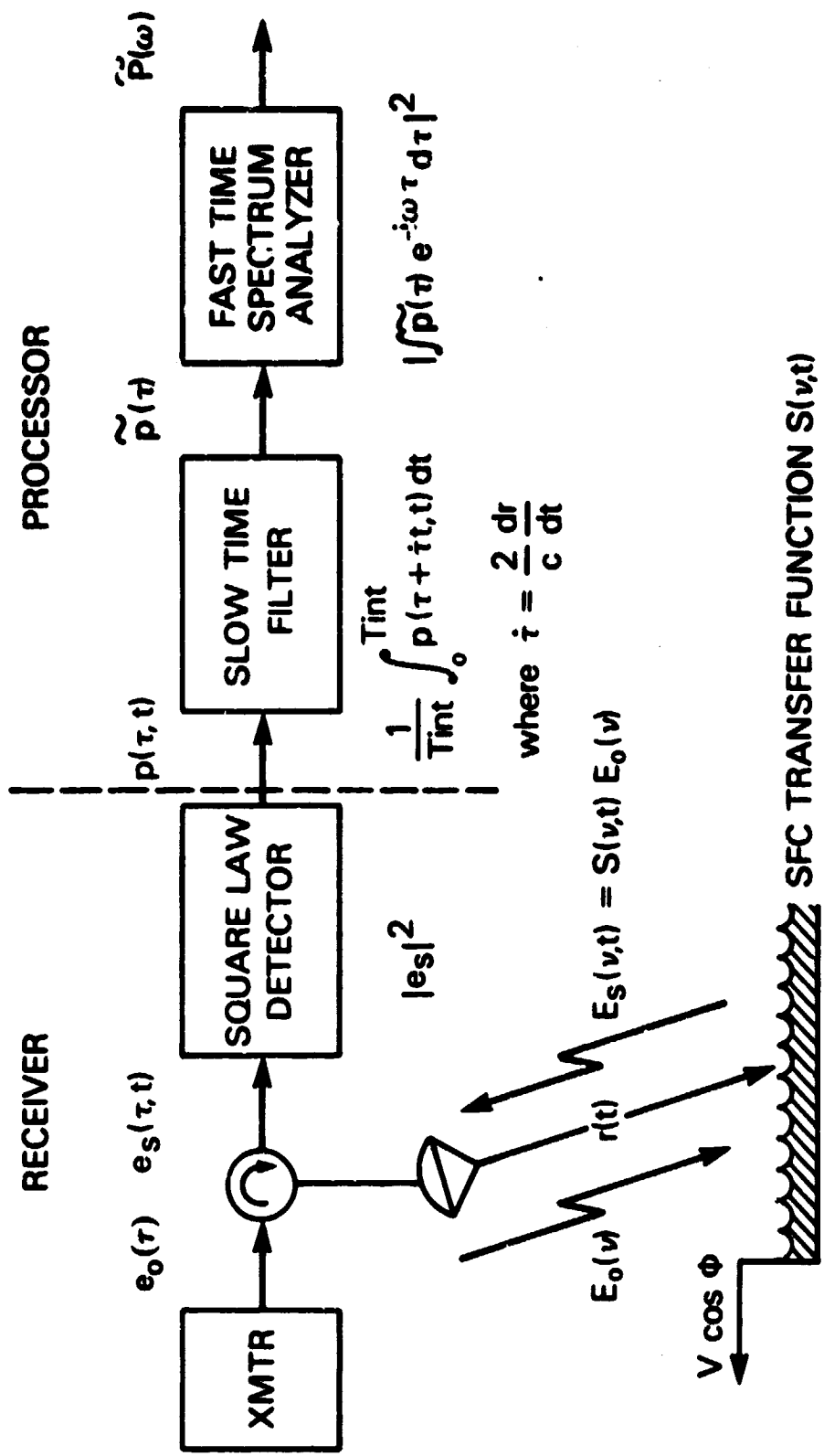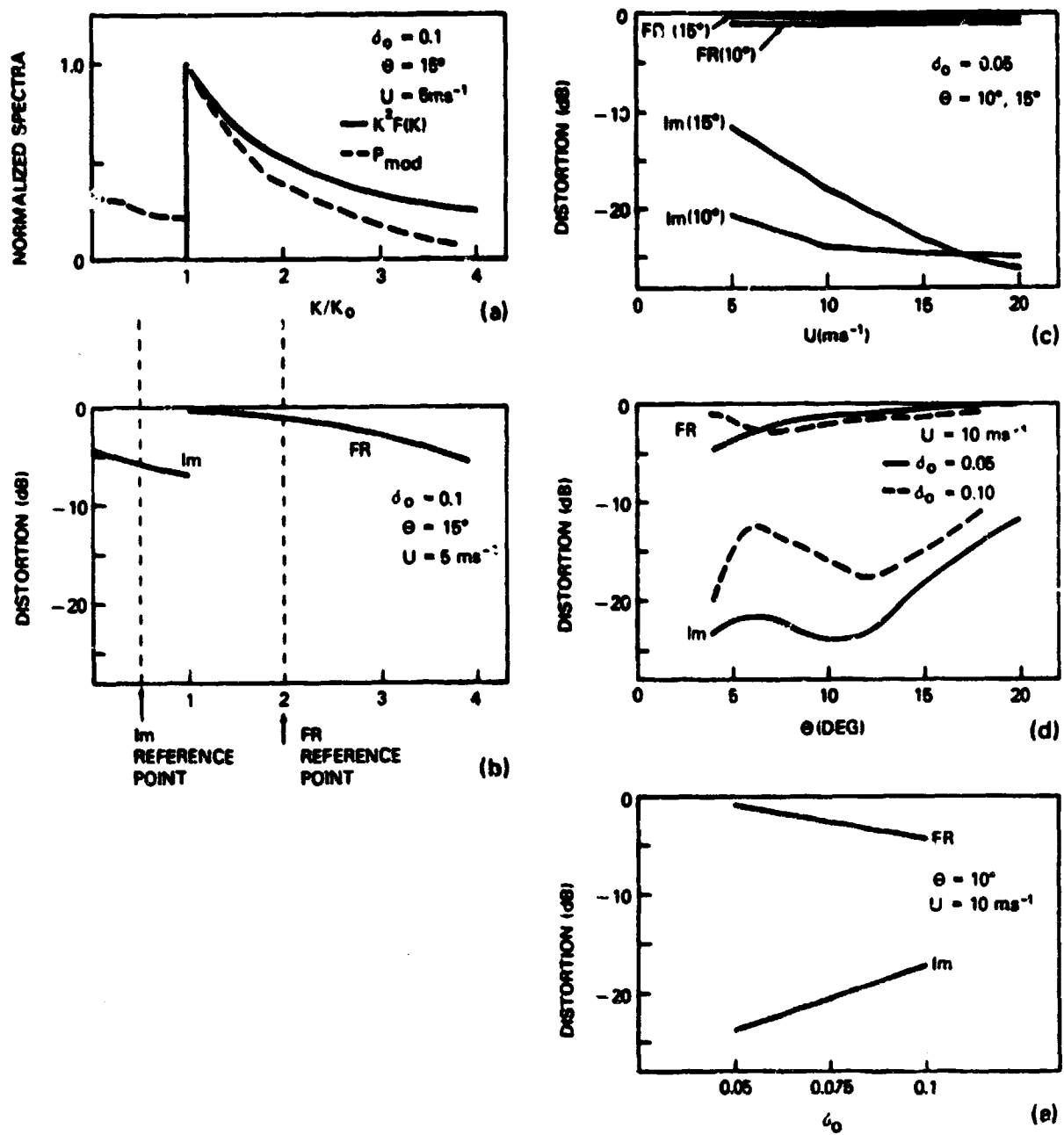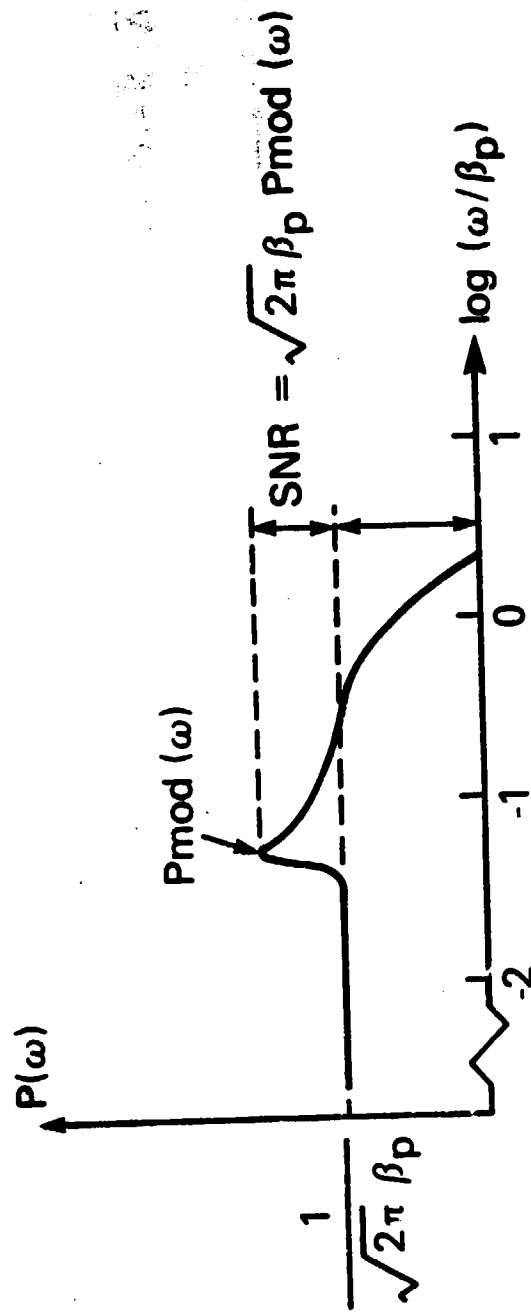
Figure 2

RECEIVER   SPECTRUM ANALYZER

(a)

RECEIVER   CORRELATOR

(b)

Figure 3

Figure 4

RECEIVER   PROCESSOR

XMTR

$e_o(\tau)$ $e_s(\tau,t)$

SQUARE LAW DETECTOR

$|e_s|^2$

$p(\tau,t)$

SLOW TIME FILTER

$$\frac{1}{T_{int}} \int_o^{T_{int}} p(\tau + \dot{\tau}t, t)\, dt$$

where $\dot{\tau} = \frac{2}{c}\frac{dr}{dt}$

$\tilde{p}(\tau)$

FAST TIME SPECTRUM ANALYZER

$$\left| \int \tilde{p}(\tau)\, e^{-i\omega\tau}\, d\tau \right|^2$$

$\tilde{P}(\omega)$

$E_o(\nu)$

$V\cos\Phi$

$r(t)$

$E_s(\nu,t) = S(\nu,t)\, E_o(\nu)$

SFC TRANSFER FUNCTION $S(\nu,t)$

52

Figure 5

Figure 6

Figure 7